Introducing The Plaid Model

Richard Evan Schwartz *

June 4, 2015

Abstract

We introduce and prove some basic results about a combinatorial model which produces embedded polygons in the plane. The model is highly structured and relates to a number of topics in dynamics and geometry.

1 Introduction

The purpose of this paper is to introduce a combinatorial model which produces embedded lattice polygons in the plane. The model is related to a variety of things: outer billiards on kites [**S1**], [**S2**], circle rotations, polyhedron exchange transformations, corner percolation, P. Hooper's Truchet tile system [**H**], and DeBruijn's theory of multigrids [**DeB**]. I call the model the *plaid model* because of the grids of parallel lines it involves.

The plaid model depends on a rational parameter $p/q \in (0,1)$, and we always [1] take pq to be even. Figure 1.1 shows some of the polygons produced by the model for the parameter $4/17$ and Figure 1.2 shows some of the polygons produced by the model for the parameter $17/72$. These parameters are successive terms in the continued fraction expansion of $\sqrt{5}-2$, a parameter which figures heavily in [**S2**]. If you look closely at these pictures you notice that the second one contains lots of copies of the polygons in the first one, and also the large polygons in the two pictures match up very well when they are rescaled to have the same size and superimposed.

* Supported by N.S.F. Research Grant DMS-1204471

[1] There is a similar kind of theory when pq is odd, but it is sufficiently different that I will not discuss it here. Also, I haven't really worked it out in detail.

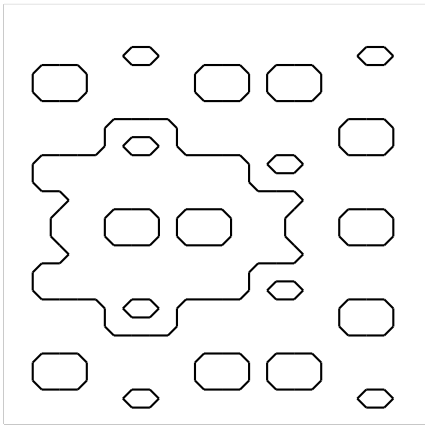

Figure 1.1: Some of the polygons for the parameter 4/17.

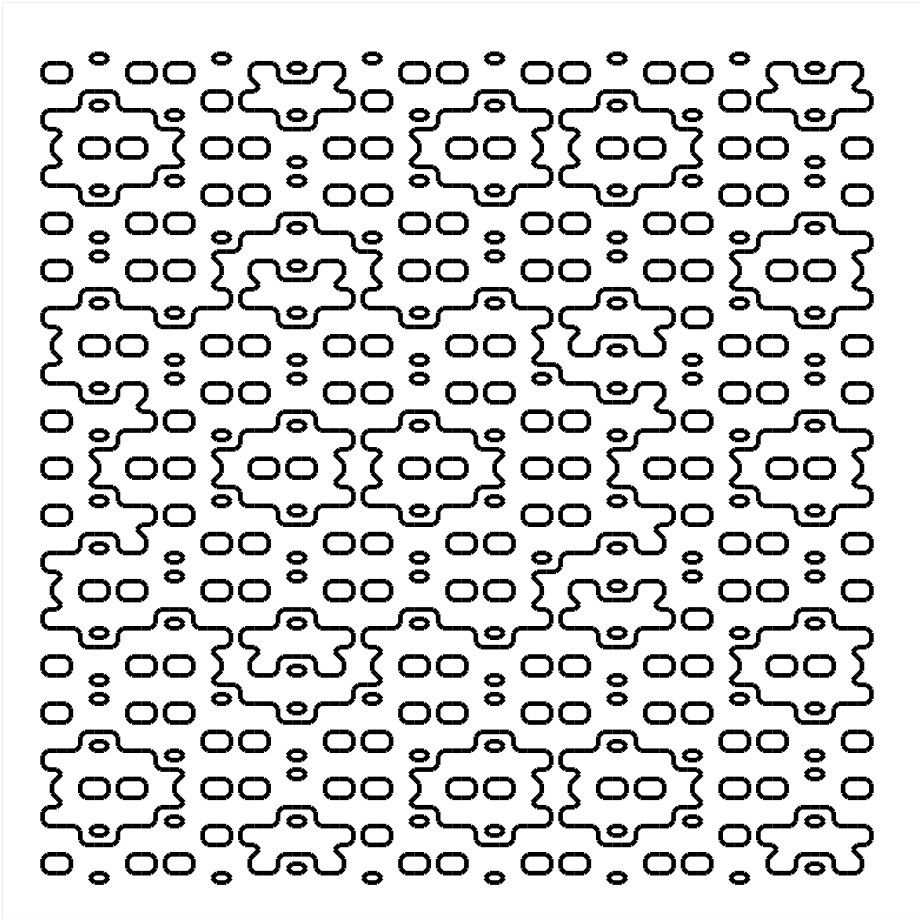

Figure 1.2: Some of the polygons for the parameter 17/72.

These kinds of phenomena are ubiquitous in the model, and hint at its depth. My main aim in this paper is to introduce the plaid model and prove some basic things about it.

I discovered the plaid model in my effort to understand the coarse self-similarity one sees in the *arithmetic graphs* associated to outer billiards on kites. There seems to be so much to say about the plaid model that I don't even get to the outer billiards connection in this paper, though I will include a brief account in §8. The plaid model is a kind of elaboration of the Hexagrid Theorem from [**S1**] but the account here is self-contained and has nothing apparently to do with outer billiards on kites. I imagine that the plaid model is something that one could study for its own sake.

Here is an overview of the paper. In §2, I will describe the plaid model in terms of the intersection points of a system of grids in the plane, and I will establish some of its basic properties. From the description, it is not at all clear why the model produces polygonal paths, or indeed anything interesting. However, the Theorem 2.1 (the Fundamental Theorem) says that the plaid model really does make sense as a generator of polygonal paths.

In §3 I will give a second description of the plaid model in terms of polyhedron exchange transformations. Here is the main result of the paper.

Theorem 1.1 (PET Equivalence) *Let p/q be an even rational parameter. Let $P = 2p/(p+q)$. The plaid polygons associated to p/q describe the vector dynamics of a set of distinguished orbits in a 3 dimensional polyhedron exchange transformation $\widehat{X}_P$. Moreover, there is a 4-dimensional fibered convex integral affine polytope exchange transformation whose fiber over P is $\widehat{X}_P$.*

All this terminology will be defined in §3. By *vector dynamics*, I mean that we associate one of the unit vectors in $\boldsymbol{Z}^2$, or the 0-vector, to each region of a polyhedron exchange transformation. Following an orbit, one obtains a sequence of vectors, which one "accumulates" to produce a polygonal path. This will make sense even at irrational parameters but when $P = 2p/(p+q)$ the vector dynamics of the distinguished orbits produces the plaid polygons with respect to the paramater p/q.

For each parameter, our PET has a flat 3 torus as its domain. This flat 3 torus has a natural subdivision into cubes of sidelength $2/(p+q)$, and the dynamics preserves the set of centers of these cubes. These are the distinguished orbits referred to in the PET Equivalence Theorem.

As we will see, the PET Equivalence Theorem immediately implies [2] the Fundamental Theorem. Moreover, the PET Equivalence Theorem allows one to extend the plaid model to irrational parameters in $(0, 1)$.

In §4 I will prove several results concerning the distribution of large orbits in the rational case. Theorems 4.1 and 4.2 are the main results. Theorem 4.2 goes beyond anything I could say about outer billiards in [**S1**], and involves a rescaled limit of the plaid model.

In §5-8 I will prove the PET Equivalence Theorem. The proof exploits the "physical nature" of the plaid model, in which certain of the intersection points are grouped into "particles" which (when suitably interpreted) move around and obey billiard-like laws.

In §9 I will explain the connection between the plaid model and outer billiards on kites. The main conjectural result, Conjecture 9.1 (The Quasi-Isomorphism Conjecture) says that the closed loops produced by the plaid model are the same, up to an error of at most 2 units, as certain affine images of the arithmetic graphs associated to outer billiards on kites.

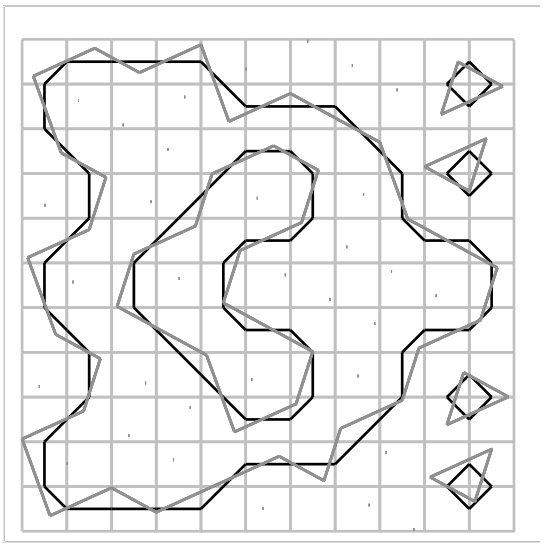

Figure 1.3: The Quasi-Isomorphism Conjecture in action for 3/8.

For the parameter 3/8, Figure 1.3 superimposes the plaid polygons in a certain region of the plane on top of the said affine images of the arithmetic graphs.

[2] Technically, we will deduce the Fundamental Theorem from Theorem 3.3, the Isomorphism Theorem, which is a precursor to the PET Equivalence Theorem.

All this terminology will be defined in §9. I believe that a generalization of my proof of the Hexagrid Theorem in [**S1**] will establish the Quasi-Isomorphism Conjecture, but the proof will require a separate paper. The Quasi-Isomorphism Conjecture (once proved) converts the plaid model into a machine for generating results about the arithmetic graphs associated to outer billiards on kites.

The paper comes with a companion computer program which illustrates many of the results in this paper - in particular the PET Equivalence Theorem. One can download this program from my website. The URL is

http://www.math.brown.edu/∼res/Java/PLAID.tar

I discovered all the results in the paper using a more sophisticated version of the program above. The more sophisticated version is too complicated for public consumption.

I would like to think Peter Doyle, Pat Hooper, Sergei Tabachnikov, and Ren Yi for a number of conversations about things related to the plaid model.

2 The Grid Description of the Plaid Model

2.1 Basic Definitions

Even Rational Parameters: We will work with $p/q \in (0,1)$ with pq even. We call such numbers *even rational parameters*. We will work closely with the auxiliary rationals

$$P = \frac{2p}{p+q}, \qquad Q = \frac{2q}{p+q}. \tag{1}$$

These rationals have the property that $P + Q = 2$ and $P/Q = p/q$.

Four Families of Lines We consider 4 infinite families of lines.

- $\mathcal{H}$ consists of horizontal lines having integer y-coordinate.
- $\mathcal{V}$ consists of vertical lines having integer x-coordinate.
- $\mathcal{P}$ is the set of lines of slope $-P$ having integer y-intersept.
- $\mathcal{Q}$ is the set of lines of slope $-Q$ having integer y-intersept.

Figure 2.1 shows these lines inside $[0,7]^2$ for $p/q = 2/5$. In this case, $P = 4/7$ and $Q = 10/7$.

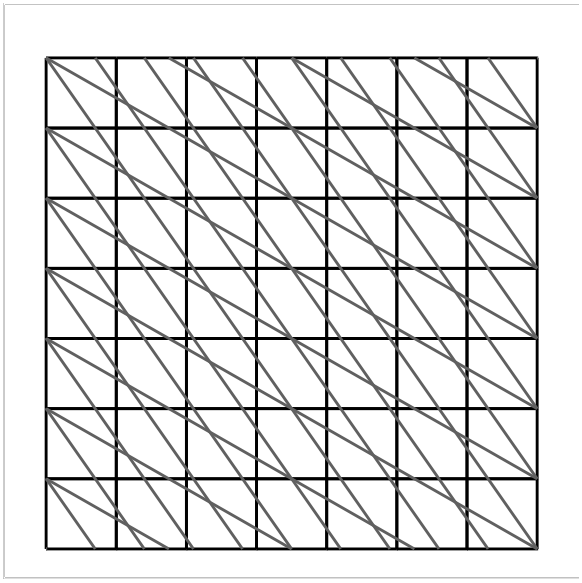

Figure 2.1: The 4 line families for $p/q = 2/5$.

Adapted Functions: Let $\boldsymbol{Z}_0$ and $\boldsymbol{Z}_1$ denote the sets of even and odd integers respectively. We define the following 4 functions:

- $F_H(x,y) = 2Py \bmod 2\boldsymbol{Z}$
- $F_V(x,y) = 2Px \bmod 2\boldsymbol{Z}$.
- $F_P(x,y) = Py + P^2x + 1 \bmod 2\boldsymbol{Z}$
- $F_Q(x,y) = Py + PQx + 1 \bmod 2\boldsymbol{Z}$.

We call F_H and F_V *capacity functions* and F_P and F_Q *mass functions*. We shall never be interested in the inverse images of $\boldsymbol{Z}_1$, so we will always normalize so that our functions take values in $(-1,1)$. Lemma 2.2 gives a geometric view of these functions, in terms of circle rotations.

Intersection Points: We set

$$\omega = p + q, \qquad \Omega_j = \boldsymbol{Z}_j\omega^{-1}. \tag{2}$$

We observe that, for each index $A \in \{H,V\}$ and $B \in \{P,Q\}$, we have $F_A^{-1}(\Omega_0) = \mathcal{A}$ and $F_B^{-1}(\Omega_1) = \mathcal{B}$.

We call z an *intersection point* if z lies on both an A line and a B line. In this case, we call z *light* if

$$|F_B(z)| < |F_A(z)|, \qquad F_A(z)F_B(z) > 0. \tag{3}$$

Otherwise we call z *dark*. We say that B is the *type* of z. Thus z can be light or dark, and can have type P or type Q. When z lies on both a $\mathcal{P}$ line and a $\mathcal{Q}$ line, we say that z has both types.

Capacity and Mass: For any index $C \in \{V,H,P,Q\}$, we assign two invariants to a line L in $\mathcal{C}$, namely $|(p+q)F_C(L)|$ and the sign of $F_C(L)$. We call the second invariant the *sign* of L in all cases. When $A \in \{V,H\}$, we call the first invariant the *capacity* of L. When $A \in \{P,Q\}$ we call the first invariant the *mass* of L. The masses are all odd integers in $[1, p+q]$ and the capacities are all even integers in $[0, p+q-1]$. Thus, our rule can be described as follows. An intersection point is light if and only if the intersecting lines have the same sign, and the mass of the one line is less than the capacity of the other.

Figure 2.2 shows the light intersection points inside the suequare $[0,7]^2$ for the parmeter $2/5$. For each unit square S in this region, we have connected the center of S to the light points on ∂S.

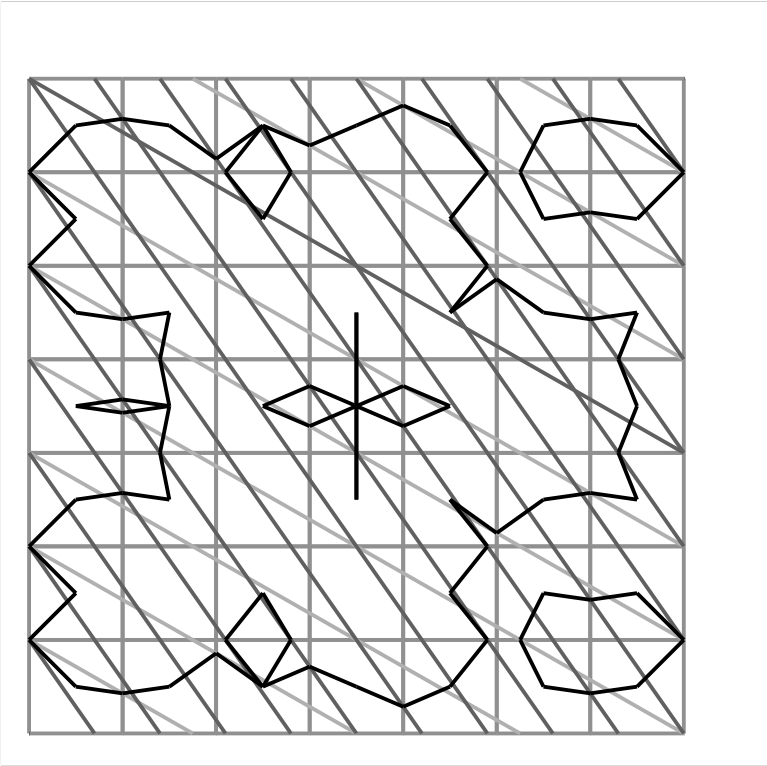

Figure 2.2: Some light points for $p/q = 2/5$.

Notice that some interesting curves seem to emerge. Notice also that there seems to be a small amount of junk (in the form of little loops) hanging off these curves. Our rule below will prune away the junk and keep the interesting part.

Double Counting Midpoints: We introduce the technical rule that we count a light point twice if it appears as the midpoint of a horizontal unit segment. The justification for this convention is that such a point is always a triple intersection of a $\mathcal{P}$ line, a $\mathcal{Q}$ line, and a $\mathcal{H}$ line; and moreover this point would be considered light either when computed either with respect to the $\mathcal{P}$ line or with respect to the $\mathcal{Q}$ line. See Lemma 2.8 below.

Good Segments: We call the edges of the unit squares *unit segments*. Such segments, of course, either lie on $\mathcal{H}$ lines or on $\mathcal{V}$ lines. We say that a unit segment is *good* if it contains exactly one light point. We say that a unit square is *coherent* if it contains either 0 or 2 good segments. We say that the plaid model is *coherent* at if all squares are coherent for all parameters. Here is the fundamental theorem concerning the plaid model.

Theorem 2.1 (Fundamental) *The plaid model is coherent for all parameters.*

Plaid Polygons: The Fundamental Theorem allows us to create a union of embedded polygons. In each unit square we draw the line segment which connects the center of the square with the centers of its good edges. The squares with no good edges simply remain empty. We call these polygons the *plaid polygons*. Figure 2.3 shows the plaid polygons contained in $[0, 7]^2$ for the parameter $2/5$.

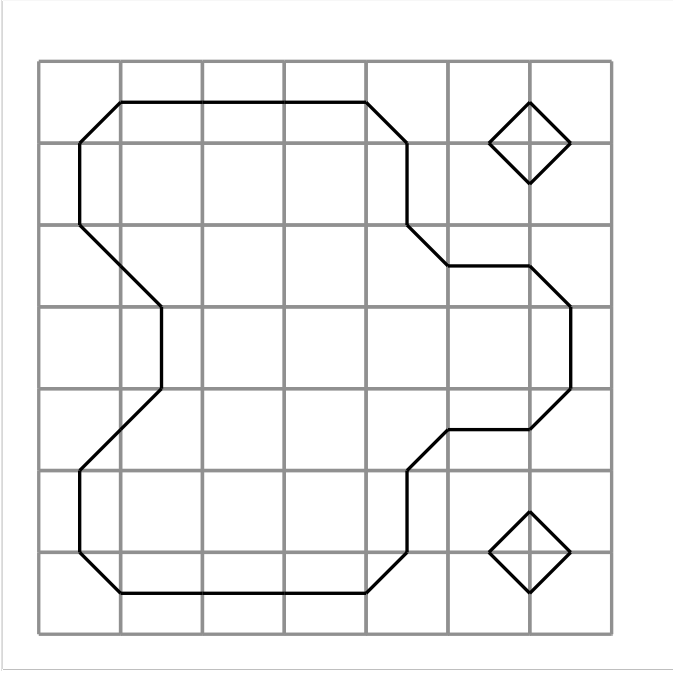

Figure 2.3: The plaid polygons inside $[0, 7]^2$ for $p/q = 2/5$.

2.2 The Tune of the Model

Given a parameter p/q let $\omega = p + q$. We solve the equation

$$2\alpha p \equiv \pm 1 \text{ mod } \omega. \tag{4}$$

and let α be which ever solution lies in $(0, \omega/2)$. We then define the *tune* of the model to be

$$\tau(p/q) = \alpha/\omega. \tag{5}$$

The numbers p/q and $\tau(p/q)$ control the geometry of the model, thanks to the following lemma.

Lemma 2.2 *For $k = 0, ..., (\omega - 1)/2$, the lines of capacity $2k$ have the form*

$$x = k\tau\omega, \qquad x = \omega - k\tau\omega, \qquad y = k\tau\omega, \qquad y = \omega - k\tau\omega.$$

For $k = 1, 3, ..., (\omega - 1)$, the the lines of mass k have y-intercepts

$$(0, k\tau\omega), \qquad (0, \omega - k\tau\omega).$$

These equations are taken mod ω.

Proof: We will deal with the line $y = k\tau\omega$ and the case $2p\alpha \equiv 1 \text{ mod } \omega$. The other cases are similar. We compute

$$F_H(0, y) = [2Pk\tau\omega]_2 = [4pk\tau]_2 = \frac{2}{\omega}[2pk\alpha]_\omega = \frac{2}{\omega}[k]_\omega = \frac{2k}{\omega}.$$

We deal with the $\mathcal{P}$ lines and $\mathcal{Q}$ lines at the same time. We will deal with the case when the y-intercept is $(0, ka)$. The other case is similar. We now are assuming that k is odd. We know that $[2Pky]_2 = 2k/\omega$. We Multiply this equation above by $\omega/2$, we see that $[2pky]_\omega = [\omega Pky]_\omega = k$. In short $2kpy \equiv k \text{ mod } \omega$. Since ω and k are odd, and $2pky$ is even, we have $2pky \equiv \omega + k \text{ mod } 2\omega$. But then

$$F_P(0, y) = [Py + 1]_2 = \frac{[\omega Pky + \omega]_{2\omega}}{\omega} = \frac{[2pyk + \omega]_{2\omega}}{\omega} = \frac{k}{\omega}.$$

Hence the $\mathcal{P}$ and $\mathcal{Q}$ lines through $(0, y)$ have mass k. ♠

The close connection between the plaid model and circle rotations suggests that there ought to be a lot of renormalization going on in the model. We will not pursue this here, though we will exploit the circle rotation property when we prove Theorem 4.2.

2.3 Symmetries

The Symmtry Lattice We fix some even rational parameter p/q. Let $\omega = p + q$ as above. Let $L \subset \boldsymbol{Z}^2$ denote the lattice generated by the two vectors

$$(\omega^2, 0), \qquad (0, \omega). \tag{6}$$

We call L the *symmetry lattice*.

Blocks: We define the square $[0, \omega]^2$ to be the *first block*. The pictures above always show the first block. In general, we define a *block* to be a set of the form $B_0 + \ell$, where B_0 is the first block and $\ell \in L$. With this definition, the lattice L permutes the blocks. We define the *fundamental blocks* to be $B_0, ..., B_{\omega-1}$, where B_0 is the first block and

$$B_k = B_0 + (k\omega, 0). \tag{7}$$

The union of the fundamental blocks is a fundamental domain for the action of L. We call this union the *fundamental domain*.

Translation Symmetry: All our functions F are L-invariant. That is, $F(v + \ell) = F(v)$ for all $\ell \in L$. This follows immediately from the definitions. Note that a unit segment in the boundary of a block does not have any light points associated to it because $F_H = 0$ on the horizontal edges of the boundary and $F_V = 0$ on the vertical edges of the boundary. (A vertex of such a segment might be a light point associated to another unit segment incident to it but this doesn't bother us.) Thus, assuming the truth of the Fundamental Theorem – so that the definition of a plaid polygon makes sense – every plaid polygon is contained in a block, and is translation equivalent to one that is contained in a fundamental block.

Rotational Symmetry: The plaid model is invaruant under reflection in the origin. Here is how we see this. For each of the functions F, we have $F(-x, -y) = -F(x, y) \bmod 2\boldsymbol{Z}$. This means that the rotation in the origin preserves the set of light intersection points and the set of dark intersection points, and preserves the types.

Reflection Symmetry: Let $\widehat{L}$ denote the group of isometries generated by reflections in the horizontal and vertical midlines (i.e. bisectors) of the

blocks. We will show through a series of lemmas that the elements of $\widehat{L}$ preserve the set of plaid polygons. However, for the reflections in horizontal lines, the vertical interection points of type P are swapped with the vertical intersection points of type Q.

The group $\widehat{L}$ is generated by L, by the rotation mentioned above, and by reflection in the x-axis. So, to finish the proof, we just have to analyze what happens for reflection in the x-axis. This is the interesting case.

Lemma 2.3 *The set of light points for the plaid model is invariant under reflection in the x-axis. This reflection preserves the type of the horizontal light points and swaps the types of the vertical light points.*

Proof: We will show that the reflection preserves a light point $z = (x, y)$ of type P. The proofs in the other cases are very similar.

Suppose first that z lies on a vertical edge. Let $z' = (x, -y)$. We have

$$F_V(z') = F_V(z), \quad F_P(z') = F_V(z) - F_Q(z) \quad F_Q(z') = F_V(z) - F_P(z). \tag{8}$$

The last two equations hold mod $2\boldsymbol{Z}$. Using the rotation symmetry, we reduce to the case when $F_P(z) > 0$. But then $F_V(z) > 0$ and $F_P(z') + F_Q(z) = F_V(z)$ when the values are forced to lie in $(-1, 1)$. Note that $\boldsymbol{Z}_0 - \boldsymbol{Z}_1 = \boldsymbol{Z}_1$. So, $F_Q(z') \in \boldsymbol{Z}_1$. But then our definitions tell us that z' is a light point of type Q.

Now suppose that z lies on a horizontal segment. We have

$$F_H(z') = -F_H(z), \quad F_P(z') - F_H(z') = F_P(z), \quad F_Q(z') - F_H(z') = F_Q(z). \tag{9}$$

Using the rotational symmetry, we can assume that

$$F_H(z) < F_P(z) < 0 \tag{10}$$

But then $F_H(z') > 0$. Equation 9 forces $F_P(z') < F_H(z')$. Equation 10 combines with the equation

$$F_P(z') = F_P(z) - F_H(z) \qquad \text{mod } 2\boldsymbol{Z}$$

to force $F_P(z') > 0$. This $0 < F_P(z') < F_H(z')$. Finally, Equation 9 tells us that $F_P(z') \in \Omega_1$. So, z' is a light point of type P. ♠

2.4 The Number of Intersection Points

The purpose of this section is to prove the following result.

Lemma 2.4 *Each unit segment contains* 2 *intersection points.*

Proof: Let e be a vertical edge. Let L be the vertical line through e. There is some $\alpha \in [0,1]$ such that the intersection points of type P along L have the form $n+\alpha$, where $n \in \boldsymbol{Z}$. The same goes for the points of type Q. Hence, there are exactly two of them in e. (This works even when $\alpha = 0$.)

Now let e be a horizontal edge. If we forget about whether the intersection points are light or dark, the whole picture is symmetric under translation by $(0,1)$ and also $(p+q,0)$. So, we can assume that e lies on the south boundary the first block. The intersection points of type P have the form $(n/P,0)$ where $n \in \boldsymbol{Z}$ and the intersection points of type Q have the form $(n/Q,0)$.

Case 1: If e is the central edge, then e contains the intersection points

$$(p/P,0) = (q/Q,0) = ((p+q)/2,0).$$

This common point is counted twice, by convention.

Case 2: If e is the westernmost edge, then e contains the two intersection points $(0,0)$ and $(1/Q,0)$. If e is the easternmost edge, then e contains $(p+q,0)$ and $(p+q,0)-(1/Q,0)$.

Case 3: If e is not one of the edges above, then neither the boundary nor the midpoint of e contains an intersection point. Since $1/Q \in (1,2)$ we know that e contains at least 1 point of type Q and at most 2 of them. We will show that if e does not contain a second point of type Q then e contains a point of type P. Let $(k_1/Q,0)$ be the point of type Q that e does contain. We must have $k_1 \in (Qm+Q-1, Qm+1)$, for otherwise we could add or subtract 1 from k_1 and produce another intersection point of type Q in e. We claim that there is some point of type P inside e. We seek a point $k_2 \in (Pm, Pm+P)$. This time we have

$$k_1 + k_2 \in (2m+Q-1, 2m+P+1) = (2m+1-P, 2m+1+P),$$

The value $k_2 = (2m+1)-k_1$ does the job. ♠

2.5 Capacity and Mass

Now we come to a more subtle result which suggests the hierarchical nature of the plaid model. The lines of small capacity have very few light points, so they predict something about the large scale geometry of the loops in the model. As we add more lines of higher capacity, the picture of the loops fills in at finer scales. We will take up this discussion in detail in §4.

Theorem 2.5 *Let B be any block. For each even $k \in [0, p+q]$ there are 2 lines in $\mathcal{H}$ and 2 lines in $\mathcal{V}$ which have capacity k and intersect B. Each such line carries k light points in B.*

Lemma 2.6 *Statement 1 of Theorem 2.5 is true.*

Proof: Recall that $\omega = p+q$. Given the periodicity of the functions F_H and F_V, it suffices to prove this for the first block. We will prove the result for $\mathcal{H}$. The result for $\mathcal{V}$ has virtually the same proof. We are simply trying to show that there are exactly 2 integer values of y in $[0, \omega]$ such that $4py = \pm k \bmod 2\omega$. Writing $k = 2h$, we see that this equation is equivalent to $2py = \pm h \bmod \omega$. This has 2 solutions mod ω because $2p$ is relatively prime to ω. ♠

Lemma 2.7 *Theorem 2.5 holds in the vertical case.*

Proof: Let L be a vertical line of capacity k. The case $k = 0$ is trivial, so we assume $k > 0$. In this case, no point of type P coincides with a point of type Q. We will show that there are $k/2$ light points of type P in $L \cap B$. By reflection symmetry, the same goes for the points of type Q.

Let $S_P \subset \boldsymbol{Z}$ denote those points m such that the line Λ_m of $\mathcal{P}$ through $(0, m)$ intersects $L \cap B$. The set S_P is the intersection of $\boldsymbol{Z}$ with a segment of length ω. When $k > 0$ this segment has endpoints which are not in $\boldsymbol{Z}$. Hence S_P consists of exactly ω consecutive integers.

The restriction of ωF_P to Λ_m is $2pm + \omega$. Choose any odd $\ell \in (0, k)$. To prove our result we just have to show that there is exactly one $m \in S_P$ such that

$$2pm + \omega \equiv \ell \qquad \bmod 2\omega$$

Since ω is odd, we can write $\ell = 2d + \omega$, and the congruence above is equivalent to $pm \equiv d \bmod \omega$. There is exactly one solution to this in any run of ω consecutive integers. ♠

Lemma 2.8 *Theorem 2.5 holds in the horizontal case.*

Proof: Let L be a horizontal line of capacity k which interects the block B. By symmetry, we can assume that B is one of the fundamental blocks. Let L_+ and L_- be the two horizontal lines of capacity k and $-k$ respectively. Reflection in the horizontal midline of B swaps these two lines.

Let $\ell \in (0,k)$ be some odd integer. Let $S(\ell)$ denote the set $x \in \boldsymbol{R}$ with the following property. There is some $y \in \boldsymbol{R}$ such that either

- (x,y) is a light point of type P on L_-.
- (x,y) is a light point of type Q on L_+.

We will show that $S(\ell)$ has cardinality 2 for all $\ell = 1, ..., k-1$. This fact, together with the bilateral symmetry, establishes the lemma.

Let S_Q (respectively $\widehat{S}_P$) denote the set $m \in \boldsymbol{Z}$ such that the line of slope $-Q$ (respectively $+P$) through $(0,m)$ intersects L_+. By symmetry, our set $S(\ell)$ has the following description. We consider all points $m \in S_Q \cup \widehat{S}_P$ having $\omega F_P(0,m) \equiv \ell \bmod 2\omega$. We then intersect the appropriately sloped line through $(0,m)$ with L_+ and record the x coordinate. We call (x, y_+) a *guide point*. Here y_+ is the y-coordinate of L_+.

We claim $\widehat{S}_P \cup S_Q$ contains numbers in every congruence class mod 2ω. Consider first the case when B is the first block. In this case, y_+ is both the right endpoint of $\widehat{S}_P$ and the left endpoint of S_Q. So, in this case, the union is a run of $2\omega + 1$ consecutive integers. So, the congruence property holds. When we replace the first block B by the kth block B', the set $\widehat{S}_P$ moves down by $2pk$ units and the set S_Q moves up by $2qk$ units. Hence, the congruence property still holds.

As in the proof of Lemma 2.8, we are trying to solve the equation

$$pm \equiv d \bmod \omega, \qquad \ell = 2d + \omega, \qquad m \in \widehat{S}_P \cup S_Q.$$

The congruence property implies that there are 2 solutions m and m' modulo 2ω.

If $m \equiv m' \bmod 2\omega$, then the corresponding giode points coincide because $P+Q = 2$ and relevant lines of slope $-Q$ and P intersect the y-axis at points which are $2k\omega$ apart. If $m \equiv m' + \omega \bmod 2\omega$ and $y_+ = (m+m')/2$ the two guide points lie at the center point of $L_+ \cap B$ and our convention says to count the point twice. In all other cases, the two guide points are distinct. ♠

2.6 Remote Adjacency and Particles

The results in the previous section are a kind of conservation principle. As we move from block to block, the number of light points on a line of capacity k (namely k of them) does not change. In this section, we further the physical analogy and explain how to think about our intersection points as moving particles. This is a key step in our proof of the Fundamental Theorem.

Let $B_0, ..., B_{\omega-1}$ be the fundamental blocks. Let $a \in (0, \omega)$ be such that

$$2ap \equiv -1 \mod \omega. \tag{11}$$

We say that the blocks B_j and B_{j+a} are *remotely adjacent*. These indices are taken mod ω. We write $B_j \to B_{j+a}$. Note that a is relatively prime to ω, so that cycle $B_0 \to B_a \to B_{2a}...$ lists out every fundamental block.

Given a fundamental block B, there is a horizontal translation T such that $T(B) = B_0$. Given any point $z \in B$, we define $[z] = T(z) \in B_0$. The point $[z]$ records the position of z within B.

Lemma 2.9 *Suppose $B \to B'$. Let H be a $\mathcal{H}$ line which intersects B and B'. Let z be an intersection point on H. Suppose z has type P (respectively type Q) and is not on the left (respectively right) edge of B. Then there is a point $z' \in B' \cap H$ of the same type and brightness such that $[z'] - [z] = (P^{-1}, 0)$ (respectively $[z'] - [z] = (-Q^{-1}, 0)$.)*

Proof: Consider first the case when z has type P. The first thing we have to do is check that $z' \in B'$. The lines in $\mathcal{P}$ intersect H in points of the form nP^{-1} for $n \in \boldsymbol{Z}$. So, z must be at least P^{-1} from the right edge of B. This gives $z' \in B'$.

Now we will show that z' is light if and only if z is light. Let L and L' respectively be the $\mathcal{P}$ lines through z and z' respectively. Let y and y' be such that $(0, y) \in L$ and $(0, y') \in L'$. The blocks B and B' differ by a horizontal translation of $a(\omega)$. Given that the lines in $\mathcal{P}$ have slope $-P = -2p/(\omega)$, we get $y' - y = 2pa + 1$. But this difference is 0 mod ω, so that function F_P gives the same value to points on L and points on L'. Now our basic criterion says that z' is light if and only if z is light.

When z has type Q, the proof is the same except that $y' - y = 2qa - 1$ and $2aq \equiv -1 \mod \omega$. ♠

In the vertical case, the situation is different because each vertical line intersects at most one fundamental block. So, we consider a family of vertical lines $\{V_k\}$ such that V_k intersects B_k in the same relative position for all $k = 0, ..., \omega - 1$. We could say that $[B_k]$ is the same line, independent of k. We write $V_k \to V_{k+a}$. For the next result, it is useful to think of our blocks as cylinders, with the tops and bottoms identified.

Lemma 2.10 *Let $B \to B'$ be fundamental blocks. Let $V \to V'$ be vertical lines which respectively intersect these blocks. Let z be an intersection point of type P (respectively type Q) on V. Then there is an intersection point $z' \in V'$ of the same type and brightness so that $[z'] = [z] + (0, 1)$ (respectively $[z'] = [z] - (0, 1)$.)*

Proof: This has the same proof as in the horizontal case. ♠

Horizontal Motion: When (z, z') satisfy the relation indicated in one of the two lemmas above, we write $z \to z'$. Consider the horizontal case first. Let z_0 be some intersection point which starts out in the left edge of a fundamental block. We write $z_0 \to ... \to z_\omega$. The points $z_0, ..., z_{2p-1}$ all have type P, and their translates $[z_0], ..., [z_{2p}]$ move east across the first block by in steps of P^{-1}. then z_{2p} lies in the right edge of its block and has type Q. The points $z_{2p}, ..., z_{\omega-1}$ all have type Q and their translates $[z_{2p}], ..., [z_{\omega-1}]$ move west across the first block by in steps of P^{-1}. After ω steps the cycle is done.

Vertical Motion: We again have the cycle $z_0, ..., z_{\omega-1}$. This time the type does not change. The translates $[z_0], ..., [z_{\omega-1}]$ move north in steps of 1 unit in the type P case, and south in steps of 1 unit in the type Q case.

Particles: We call the points $z_0, ..., z_{\omega-1}$ comprising these cycles *particles*. We call each of the individual points z_i *instances* of the particle. So, a particle consists of all its instances. Thus, a particle consists of ω intersection points. These points are all either light or dark, and so we can speak of *light particles* and *dark particles*. The horizontal particles have points of both types, depending on their direction of motion, and the vertical particles have points all of the same type. If ω is large and we rescale the picture so that the individual blocks have unit size, the "movement" of the particles as we cycle through the blocks looks very much like locally linear motion.

3 The Tile Description of the Plaid Model

3.1 Classifying Pairs

Tiles and Connectors: Let Q be a unit square in the usual square grid. We label the edges of Q, in the obvious way, with the letters N(orth), S(outh), E(ast), and W(est). There are 7 ways to draw an edge from the midpoint of one edge of Q to the midpoint of another edge One of the ways is that we simply draw no edge at all, and the other 6 ways correspond to unordered pairs in the set $\{N, S, E, W\}$. By way of example, we say that the *NW-tile* is the one which has an edge joining the N edge to the W edge. We say that an *empty tile* is a tile with no edge drawn. In the 6 cases when we actually draw something, we call this segment a *connector*.

Coherent Tilings: Suppose that we have two adjacent tiles sharing a common edge. We say that these tiles *match* if the common edge is involved in the connectors of both tiles, or in neither. Suppose we have a tiling of the plane which uses the various tiles. We call the tiling *coherent* if every pair of adjacent tiles match across their common edge.

Classifying Spaces: We say that a *classifying space* is an convex polytope which has been partitioned into a finite number of smaller convex polytopes, each of which has been given one of 7 labels corresponding to the different types of tiles. By *partition* we mean that the polytopes have pairwise disjoint interiors. We call the classifying space *integral* if every convex polytope in sight is an integer convex polytope - i.e., the convex hull of a finite union of integer vectors.

Classifying Pairs: Recall that $\boldsymbol{Z}_1$ is the set of odd integers. Let $\mathcal{C}$ denote the set of centers of squares in the usual square grid. The points of $\mathcal{C}$ have the form $(a/2, b/2)$ where $a, b \in \boldsymbol{Z}_1$. Let X be a classifying space and let $\Xi : \boldsymbol{R}^2 \to X$ be a map. We call Ξ a *classifying map* if

- f is entirely defined on $\mathcal{C}$.
- f maps $\mathcal{C}$ into the union of interiors of the pieces of the partition.

We say that (Ξ, X) is a *classifying pair*.

3.2 Description of the Space

We fix $P \in [0,1]$ and let Λ_P denote the lattice generated by the vectors

$$(0,2,P,P), \qquad (0,0,2,0), \qquad (0,0,0,2). \tag{12}$$

The action on the first coordinate is trivial.

We take the quotient

$$X_P = (\{P\} \times \boldsymbol{R}^3)/\Lambda_P. \tag{13}$$

The cube $\{P\} \times [-1,1]^3$ serves as a fundamental domain for the action of Λ_P on $\{P\} \times \boldsymbol{R}^3$. However, the boundary identifications depend on P.

We define

$$X = \bigcup_{P \in [0,1]} X_P. \tag{14}$$

X is a flat affine manifold. Let $\widehat{\Lambda}$ denote the abelian group of affine transformations $\widehat{\Lambda} = \langle T_1, T_2, T_3 \rangle$, where

1. $T_1(x_0,x_1,x_2,x_3) = (x_0, x_1+2, x_2+x_0, x_3+x_0)$.
2. $T_2(x_0,x_1,x_2,x_3) = (x_0, x_1, x_2+2, x_3)$.
3. $T_3(x_0,x_1,x_2,x_3) = (x_0, x_1, x_2, x_3+2)$.

Then

$$X = ([0,1] \times \boldsymbol{R}^3)/\widehat{\Lambda}. \tag{15}$$

$[0,1] \times [-1,1]^3$ serves as a fundamental domain for X.

We have a map

$$\Xi : [0,1] \times \boldsymbol{R}^2 \to X, \tag{16}$$

defined by

$$\Xi(P,x,y) = (P, 2Px+2y, 2Px, 2Px+2Py) \mod \Lambda_P. \tag{17}$$

When the choice of P is understood, we will think of Ξ_P as a map from $\boldsymbol{R}^2$ into X_P. Sometimes we will drop off the first coordinate, namely P, and think of X_P as a subset of $\boldsymbol{R}^3$. For each even rational parameter p/q we set $P = 2p/(p+q)$, as above, and restrict Ξ_P to the set $\mathcal{C}$ of square tiles.

3.3 Checkerboards

Now that we have described our classifing map and the classifying space, we need to describe the partition of the classifying space. As a prelude, we describe a certain family of partitions of the square $[-1,1]^2$. The decomposition is based on a triple $U = (u_1, u_2, u_3)$ of numbers

$$-1 \le u_1 \le u_2 \le u_3 \le 1 \tag{18}$$

and also on a 4×4 "permutation matrix" M whose nonzero entries are replaced by the symbols N,S,E,W. This "matrix" is just a combinatorial object for us. It is useful to think of the triple of numbers as being pairwise distinct, and we will draw pictures this way. The cases when some of them coincide, or equal ± 1, are degenerate limits.

Forgetting about the symbols, our matrix will always be symmetric with respect to the diagonal line of slope 1. Also, there is a relation between M and U that is best discussed after the construction. Here is the 3-step construction.

1. We partition $[-1,1]^2$ into a 4×4 checkerboard by inserting the lines $x = u_1, u_2, u_3$ and also the lines $y = u_1, u_2, u_3$.

2. There are 4 squares of the grid which correspond go the nonzero entries of M. We label these according to the symbols in M. We call these the special rectangles.

3. In the row and column of a given special rectangle, we add the symbol corresponding to that rectangle. Thus, each of the other 12 rectangles is labeled by an unordered pair of symbols from $\{N, S, E, W\}$.

Compatibility: M and U must be compatible in the sense that the 4 special rectangles are squares.

As an illustration, consider the input data

$$(u_1, u_2, u_3) = (-2/3, 0, 1/3), \qquad M = \begin{bmatrix} 0 & 0 & 0 & W \\ N & 0 & 0 & 0 \\ 0 & E & 0 & 0 \\ 0 & 0 & S & 0 \end{bmatrix}.$$

For this choice of M, the compatibility condition is that $-u_1 - u_2 + u_3 = 1$. Here is the partition we get.

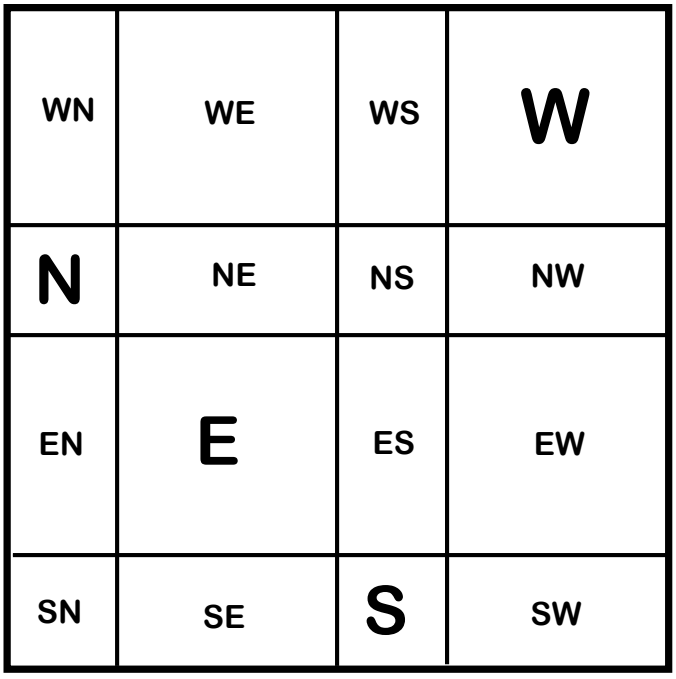

Figure 3.1: The checkerboard partition

For each choice M, we can consider the set U_M of all triples which are compatible with M. In the example above, and in all the cases considered below, U_M is a triangle with integer vertices. We think of the product

$$U_M \times [-1,1]^2 \tag{19}$$

as a fiber bundle over U_M. In each fiber we make the checkerboard construction. The union of all subsets having the same label is an integer convex polytope, and $U_M \times [-1,1]^2$ is also an integer convex polytope. We denote this space by $\langle M \rangle$

3.4 Description of the Partition

We will describe our partition of X in terms of subsets of the fundamental domain $[0,1] \times [-1,1]^3$. The coordinates we use on X are (P, T, U_1, U_2).

Let X_{PT} denote the 2 dimensional slice obtained by holding P and T fixed. Our partition is such that X_{PT} has a checkerboard partition, as discussed above. Now we will specify the parameters for the checkerboard partition as functions of P and T.

There are 3 separate ranges, so we will describe 3 sets of data.

$$T \in [\text{–}1,\text{–}1{+}P] : \quad U = (T, 1{-}P, 2{-}P{+}T), \quad M = \begin{bmatrix} 0 & 0 & 0 & W \\ N & 0 & 0 & 0 \\ 0 & E & 0 & 0 \\ 0 & 0 & S & 0 \end{bmatrix}. \tag{20}$$

$$T \in [\text{–}1{+}P, 1{-}P] : \quad U = (\text{–}1{+}P, T, 1{-}P), \quad M = \begin{bmatrix} N & 0 & 0 & 0 \\ 0 & 0 & E & 0 \\ 0 & W & 0 & 0 \\ 0 & 0 & 0 & S \end{bmatrix}. \tag{21}$$

$$T \in [1{-}P, 1] : \quad U = (\text{–}2{+}P{+}T, \text{–}1{+}P, T), \quad M = \begin{bmatrix} 0 & N & 0 & 0 \\ 0 & 0 & W & 0 \\ 0 & 0 & 0 & S \\ E & 0 & 0 & 0 \end{bmatrix}. \tag{22}$$

We can picture the data by fixing some value of P and plotting the graphs of the functions (u_1, u_2, u_3) as a function of T. Figure 3.2 shows the picture for three values of P. Here Q is such that $P + Q = 2$.

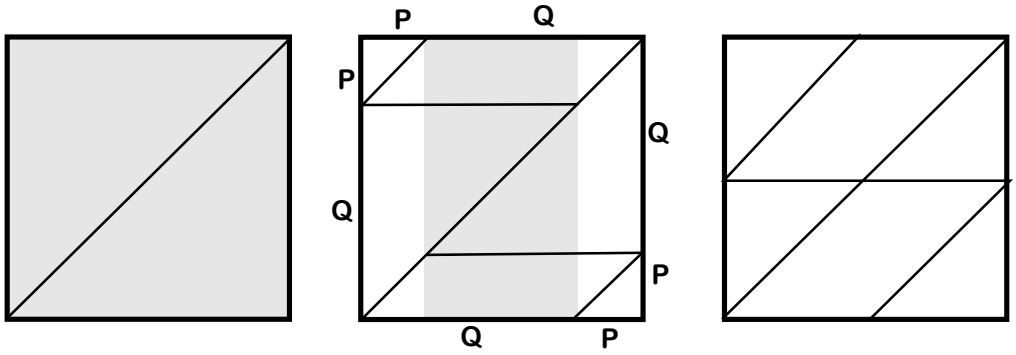

Figure 3.2: The checkerboard data for $P = 0$ and $P = 1/2$ and $P = 1$.

The space X is partitioned into 7 regions. 6 of the pieces are obtained as follows: We choose some label such as NW, and consider the union, over all fibers, of the rectangles having the label NW. We call this piece X_{NW} and we give similar names to the other pieces. What remains is X_0.

If we restrict P to $(0,1)$, the partition, combinatorially speaking, has a product structure. There are no vertices at all. When $P = 0$ the only vertices occur when $T \in \{-1, 1\}$. When $P = 1$ the only vertices occur when $T \in \{-1, 0, 1\}$. Here is a list of all the vertices.

vertices

- $(0, a, b, c)$, $\quad a, b, c \in \{-1, 1\}$.
- $(1, a, b, c)$, $\quad a, b, c \in \{-1, 0, 1\}$.

By studying Figure 3.2 we can reconstruct each individual polytope. There are 16 total, and each one intersects the generic fiber in a rectangle. Indeed, each polytope is itself the closure of a "rectangle bundle" over an open triangle.

Here is another way to think about it. Recall that X is segmented into 3 "zones", depending on the relevant values of T with respect to P, as in Equations 20 - 22. Each zone has a matrix M attached it. The linear isomorphism

$$(P, T, U_1, U_2) \to (U, U_1, U_2) \tag{23}$$

maps each zone isomorphically to $\langle M \rangle$, for the relevant choice of M. Here U is the triple in the relevant choice of Equation 20, Equation 21 or Equation 22.

3.5 Well Definedness

In this section, we explain why our classifying pair (Ξ, X) produces a well-defined tiling for each even rational parameter p/q. The issue is that perhaps Ξ maps some tile center into the boundary of the partition. We will rule this out, and in fact will prove somewhat more about the map.

Let $\omega = p + q$ and $P = 2p/\omega$. We will usually drop the reference to the parameter in our notation. Also, we will forget the P coordinate and work in $\boldsymbol{R}^3$. Recalling that $\boldsymbol{Z}_0$ and $\boldsymbol{Z}_1$ respectively denote the set of even and odd integers, we define

$$\mathcal{X} = \Big(\frac{\boldsymbol{Z}_1}{\omega}, \frac{\boldsymbol{Z}_0}{\omega}, \frac{\boldsymbol{Z}_0}{\omega}\Big). \tag{24}$$

Note that the lattice Λ consists entirely of vectors in $(\boldsymbol{Z}_0/\omega)^3$. Hence Λ preserves $\mathcal{X}$. Recall that L is the lattice of symmetries of the plaid model, and Ξ is well defined on the quotient $\mathcal{C}/L$.

Lemma 3.1 $\Xi : \mathcal{C}/L \to \mathcal{X}/\Lambda$ *is a bijection.*

Proof: Let $c \in \mathcal{C}$. We have

$$c = (x, y), \qquad x = m + 1/2, \quad y = n + 1/2, \quad m, n \in \boldsymbol{Z}.$$

Looking at the formula in Equation 17, we see that $\Xi(c) \in \mathcal{X}$.

Now $\mathcal{C}/L$ and $\mathcal{X}/\Lambda$ both have ω^3 points. The idea is that $[0, \omega^2] \times [0, \omega]$ is a fundamental domain for L and $[-1, 1]^3$ is a fundamental domain for Λ. Given the equality in the number of points of the domain and range, we just need to show that Ξ is an injection from one set into the other.

Suppose that $\Xi(c_1) = \Xi(c_2)$. We write

$$c_2 - c_1 = (x, y) = \Big(\frac{m}{\omega}, \frac{n}{\omega}\Big), \qquad m, n \in \boldsymbol{Z}. \tag{25}$$

We have

$$\Psi(c_2) - \Psi(c_2) = \Big(\frac{2pm}{\omega^2}, \frac{2pm}{\omega^2} - \frac{pn}{\omega^2}, \frac{2pm}{\omega^2} - \frac{Pn}{\omega^2}\Big) \mod \Lambda.$$

In order for the first coordinate to vanish mod Λ, we must have $m \equiv 0 \bmod \omega^2$. For the second and third coordinates to vanish mod Λ, we must have $n \equiv 0 \bmod \omega$. But then $c_2 - c_1 \in L$. ♠

So, $\Xi(\mathcal{C})$ intersects X only in the fibers above $T \in \boldsymbol{Z}_1/\omega$, and the coordinates of the image are in $\boldsymbol{Z}_0/\omega$.

Lemma 3.2 *The fiber over* $T \in \boldsymbol{Z}_1/\Omega$ *intersects the walls of the partition in lines of the form* $x = u$ *and* $y = u$ *with* $u \in \boldsymbol{Z}_1/\omega$.

Proof: When $T = -1$, the values of u are $\{-1, 1 + P, 1\}$, all of which belong to $\boldsymbol{Z}_1/\omega$. As the value of T changes by $2/\omega$, the offsets for the wall-fiber intersections change by $\pm 2/\omega$. ♠

Combining our two results, we see that $\Xi(\mathcal{C})$ never hits a wall of the partition. Hence (Ξ, X) yields a well-defined tiling.

If we place a cube of side length $2/\omega$ around each point of $\mathcal{X}$, then these cubes tile $\boldsymbol{R}^3$. Moreover, these cubes intersect each fiber over $T \in \boldsymbol{Z}_0/\omega$ in a $\omega \times \omega$ grid which exactly fills the square $[-1, 1]^2$. The image $\Xi(\mathcal{C})$ intersects this grid at the centers of the squares whereas the walls of the partition intersect the grid in line segments extending the edges of the squares.

3.6 The Isomorphism Theorem

The theorem in this section is a precursor to the PET Equivalence Theorem. In the next chapter we will deduce the PET Equivalence Theorem from the result here. Referring to the grid description of the plaid model, we define the *grid light set* of a square tile Q to be the set of edges with one light particle in them. We define the *tile light set* of a square tile to be the set of edges involved in its connector. Here is the main result of the paper.

Theorem 3.3 (Isomorphism) *For any even rational parameter and any integer unit square, the grid light set coincides with the tile light set.*

The Fundamental Theorem for the plaid model is an immediate consequence. From the tile description, the tile light set for any square has 0 or 2 members. Hence, so does the grid light set. Since the grid and light sets coincide, the equality of the two systems immediately implies that the tiling produced by our classifying pair is coherent.

3.7 Symmetries of the System

The tiling produced by our classifing pair is clearly invariant under the lattice L discussed in the previous section. Here we show that it is also invariant under the larger group $\widehat{L}$ of symmetries of the plaid model. As in §2.3 It suffices to prove that reflection in the origin is a symmetry, and that reflection in the x-axis is a symmetry.

Lemma 3.4 *The tiling produced by (Ξ_P, X) is symmetric with respect to reflection in the origin.*

Proof: We set $\Xi = \Xi_P$ and we drop the first parameter. Thus, we think of Ξ as a map from $\boldsymbol{R}^2$ into $\boldsymbol{R}^3$. Define

$$\rho(x,y) = (-x,-y), \qquad \Psi(T,U_1,U_2) = (-T,-U_1,-U_2)$$

It follows directly from the formulas that $\Xi(-x,-y) = -\Xi(x,y)$. At the same time, Ψ preserves our partition of X and permutes labels according the following scheme: N and S are swapped and E and W are swapped. But that means that ρ maps the tile centered at c to the tile centered at $\rho(c)$. ♠

Lemma 3.5 *The tiling produced by (Ξ_P, X) is symmetric with respect to reflection in the x axis.*

Proof: We make the same notational conventions as in the previous proof. This time define $\rho(x,y) = (x,-y)$ and $\Psi(T,U_1,U_2) = (T,U_2,U_1)$. We compute easily that $\Xi \circ \rho = \Psi \circ \Xi$, when these maps are restricted to points (x,y) with y a half integer. This set contains $\mathcal{C}$. At the same time, Ψ preserves our partition (and indeed each fiber) and permutes the labels by swapping N and S and doing nothing to E and W. But that means that ρ maps the tile centered at c to the tile centered at $\rho(c)$. ♠

3.8 Some Additional Formulas

We fix p/q and set $P = 2p/(p+q)$ as usual. For the purposes of calculation, it is useful to have formulas for Ξ_P which take values in the fundamental domain $\{P\} \times [-1,1]^3$. We use the coordinates (T,U_1,U_2) discussed above. Let $[x]_2$ denote the value of x mod $2\boldsymbol{Z}$ that lies in $[-2,2)$.

$$T(x,y) = [2Px+1]_2. \tag{26}$$

$$b(x,y) = \frac{1}{2}PT(x,y). \tag{27}$$

$$U_1(x,y) = [PQx + b(x,y) - Py]_2. \tag{28}$$

$$U_2(x,y) = [PQx + b(x,y) + Py]_2. \tag{29}$$

Lemma 3.6 $\Xi = (P,T,U_1,U_2) \mod \Lambda$.

Proof: On $\mathcal{C}$, the map $T(x,y)$ agrees with

$$T'(x,y) = [2Px + 2y]_2,$$

because the coordinates of points in $\mathcal{C}$ are odd half-integers. So, it suffices to check that $\Xi = (P,T',U_1,U_2)$ mod Λ. One can check that right hand side of this equation respects the identifications on $[-1,1]^3$ and gives a locally affine map into X_P. Next, using the identity $PQx + P^2x = 2Px$, one can check the equation for an open subset of $\boldsymbol{R}^2$ in which $[2Px+1]_2 = 2Px+1$. But then the equality always holds, by analytic continuation. ♠

3.9 Irrational Limits

The classifying pair (Ξ_P, X) makes sense even when P is irrational. However, it might not happen that this map gives a well-defined tiling. In this irrational case,

$$\Xi_P(1/2, 1/2) = (-1 + P, 0, P), \tag{30}$$

and this is a point in the boundary of the partition.

To remedy this situation, we introduce an *offset*, namely a vector $V \in \boldsymbol{R}^3$, and we define

$$\Xi_{P,V} = \Xi_P + (0, V). \tag{31}$$

(The first coordinate, namely P, does not change.) Since Λ_P acts on $\boldsymbol{R}^3$ with compact quotient, we can take V to lie in a compact subset of $\boldsymbol{R}^3$ and still we will achieve every possible map of this form. Since the boundary of our partition has measure 0, almost every choice of V leads to a classifying pair that defines a well-defined tiling. In this case, we call V a *good offset*.

Lemma 3.7 (Geometric Limit) *Let V be a good offset for Ξ_P. Then the tiling defined by (Ξ_P, X) is coherent.*

Proof: The proof just amounts to taking a limit of the coherence in the rational case. Let $\{p_k/q_k\}$ be a sequence of even rational parameters so that $P_k \to P$. Here $P_k = 2p_k/(p_k + q_k)$. Given any vector $W_k \in \boldsymbol{Z}^2$, we define

$$\Xi_P^{W_k}(c) = \Xi_{P_k}(c - W_k). \tag{32}$$

Since Ξ_P is locally affine, there is some other vector $V_k \in \boldsymbol{R}^3$ such that

$$\Xi_{P_k}^{W_k} = \Xi_{P_k, V_k}. \tag{33}$$

We can choose the vectors $\{W_k\}$ so that the vectors V_k converge to our offset V.

Suppose that τ_1 and τ_2 are two adjacent square tiles. Let c_1 and c_2 be the corresponding centers. By definition $\Xi_{P,V}$ maps both these centers into the interiors of pieces of our partition. By continuity, Ξ_{P_k,W_k} also maps these centers into the interiors of the same pieces, once k is sufficiently large. But that means that the tile types are the same for τ_1 and τ_2, with respect to either P_k or P. Since the tiling is coherent for (Ξ_{P_k}, X), the tiles τ_1 and τ_2 match across their boundaries. ♠

4 The Distribution of Polygons

4.1 Overview

The first main goal is to prove the following result.

Theorem 4.1 *Let $\{p_k/q_k\} \subset (0,1)$ be any sequence of even rational numbers with an irrational limit. Let $\{B_k\}$ be any sequence of associated blocks. Let N be any fixed integer. Then the number of distinct plaid polygons in B_k and the maximum diameter of a plaid polygon in B_k both exceed N for all k sufficiently large.*

When we know more about the sequence, we can get more information. We say that $\{p_k/q_k\}$ is *tuned* if the sequence $\{\tau(p_k/q_k)\}$ also converges. We call $\lim \tau(p_k/q_k)$ the *tuned limit* of the seguence. By compactness, every sequence has a tuned subsequence. We call the tuned sequence *(ir)rationally tuned* if the tuned limit is (ir)rational.

We say that the *x-diameter* of a planar set is the diameter of its projection to the x-axis. This quantity has a dynamical interpretation; see §9.3.

Theorem 4.2 *Let $\{p_k/q_k\} \subset (0,1)$ be any irrationally tuned sequence. Let $\{B_k\}$ be any sequence of associated blocks. Let N be any fixed integer. Then there is some $\delta > 0$ such that the following property holds once k is sufficiently large: At least N distinct plaid polygons have x-diameter at least $\delta\omega_k$, and every point of B_k is within ω_k/N of one of them.*

4.2 One Large Polygon

The result in this section is just a warm-up. Let p/q be an even rational parameter and let $\omega = p + q$.

Theorem 4.3 *Let B denote the first block. Then there exists a plaid polygon in B whose x-diameter is at least $\omega^2/(2q) - 1$. Moreover, this polygon has bilateral symmetry with respect to reflection in the horizontal midline of B.*

Proof: Let L be the horizontal line of capacity 2 and positive sign which intersects B. Let $z_1 = (0, y) \in L$. By Lemma 2.2, we know that z_1 is a light point of mass 1. We compute that $F_Q(z_2) = 1/\omega$, when $z_2 = (\omega^2/2q, y)$. Hence z_2 is another light point on L. Since L has capacity 2, these are

the only two light points on L. The lattice polygon which crosses the unit horizontal segment containing z_1 must also cross the unit horizontal segment containing z_2 because it has to intersect $L \cap B$ twice. This gives the lower bound on the x-diameter.

Let Γ' denote the reflection of Γ in the horizontal midline of B. We want to show that $\Gamma' = \Gamma$. Let V_1 and V_2 denote the two vertical lines of B having capacity 2. These lines are symmetrically placed with respect to the vertical midline of B. Hence, one of the two lines, say V_1, lies less than $\omega/2$ units away from the y-axis. Since $\omega/2 < \omega^2/(2q)$, the point z_2 is separated from the y-axis by V_1. Hence both Γ and Γ' intersect V_1. Since there can be at most 1 plaid polygon which intersects $V_1 \cap B$, we must have $\Gamma = \Gamma'$. ♠

4.3 The Empty Rectangle Lemma

Fixing a parameter p/q and a block B and an even integer $K \geq 0$ let Γ_K denote the union of all the lines of capacity at most K which intersect B. The complement $B - \Gamma_K$ consists of $(K+1)^2$ rectangles arranged in a grid pattern. We say that one of these rectangles is *empty* if its boundary has no light points on it. Empty rectangles serve as barriers, separating the plaid polygons inside them from the plaid polygons outside them.

Lemma 4.4 *For all parameters, all blocks B, and all choices of K, at least one of the rectangles of $B - \Gamma_K$ is empty.*

Proof: This is a counting argument. We will suppose that there are no empty boxes and derive a contradiction. There are a total of $(K+1)^2$ rectangles. If some rectangle R has a light point on it, then it must have a second light point, because the polygon Γ crossing into R through an edge containing one of the light points must cross out of R through another edge.

The one exceptional situation is when the light point z lies at the corner of R. In this case, one of the edges E of R lies in a vertical boundary of the block B. Let's consider the case when E lies in the west boundary of R and z is the south west corner. The other cases are similar. Γ crosses into R through the south edge of R, but then it cannot exit through E because E lies in the boundary of B. So, even in this exceptional case, there must be 2 light points in the boundary of R.

If every rectangle has at least 2 light points, then there are at least $(K+1)^2$ light points total. The idea is that we double the number of squares but then observe that we have counted some of the points twice.

On the other hand, we know that a line of capacity k contains at most k light points. Since there are 4 lines of capacity k for each $k = 0, 2, ..., K$, this gives a total of

$$8\sum_{k=1}^{K/2} k = (K+1)^2 - 1.$$

We have one fewer point than we need. This is a contradiction. ♠

4.4 No Big Gaps

Lemma 4.5 *Let $\{p_k/q_k\} \subset (0,1)$ be any sequence of even rational numbers with an irrational limit. Then there is some fixed number R with the following property. If $p_k \in B_k$ is any point then the disk of radius R about p_k intersects at least one plaid polygon in B_k associated to p_k/q_k.*

Proof: We use the tile description of the plaid model. Let $P_k = 2p_k/(p_k+q_k)$. Since $\lim p_k/q_k$ converges, so does $\lim P_k$. Let $R = \lim P_k$. Consider the maps

$$\Xi'_{P_k}(z) = \Xi_{P_k}(z - p_k). \tag{34}$$

There are translation vectors V_k so that

$$\Xi'_{P_k} = \Xi_{P_k} + V_k. \tag{35}$$

Here Ξ_{P_k} is the map described in §3.2. Since the lattice Λ_{P_k} acts on $\boldsymbol{R}^3$ with compact quotient, we can take $\{V_k\}$ to be a bounded sequence of vectors.

By compactness, there is some limit map

$$\Xi'_R = \lim \Xi'_{P_k}. \tag{36}$$

The limit map Ξ'_R differs from the classifying map described in §3.2 by a translation. If this lemma is false, then $\Xi'_R(\mathcal{C})$ is contained entirely inside the portion of the partition which assigns trivial tiles to the squares. But on the other hand, from our work in §3.5, we can take a limit and see that $\Xi'_R(\mathcal{C}$ is dense in the classifying space X_R. This contradicts the definition of our partition where all the pieces of the partition have positive volume at all parameters. ♠

4.5 Some Congruence Lemmas

The following lemmas will be helpful in the next section.

Lemma 4.6 *Let $\{p_k/q_k\}$ be a sequence of rational numbers with an irrational limit. Then it is impossible to find uniformly bounded integers $\alpha_k, \beta_k, \gamma_k$ so that $p_k\alpha_k + q_k\beta_k = \gamma_k$.*

Proof: Let r be the limit of our sequence. Passing to a subsequence, we can assume that α, β, γ are independent of k. Dividing by q_k and taking a limit, we see that

$$r = \lim_{k\to\infty} \frac{\gamma/q_k - \beta}{\alpha} = -\beta/\alpha.$$

Hence r is rational. This is a contradiction. ♠

As usual, let $\omega = p + q$, for any even rational parameter p/q.

Lemma 4.7 *Let $\{p_k/q_k\}$ be a sequence of rational numbers with an irrational limit. Let a_k be such that $2p_ka_k \equiv -1$ mod ω_k. Then there does not exist a uniformly bounded integer sequence $\{b_k\}$ so that $2a_kb_k$ is uniformly bounded mod ω_k.*

Proof: Suppose that the sequence $\{b_k\}$ exists. Then we have another uniformly bounded integer sequence $\{c_k\}$ so that

$$2a_kb_k \equiv \quad c_k \mod \omega_k.$$

Multiplying through by p_k we get

$$-b_k \equiv c_kp_k \mod \omega_k.$$

But then

$$c_kp_k = d_k(\omega_k) - b_k,$$

for some uniformly bounded sequence $\{d_k\}$. Since $\omega_k = p_k + q_k$, we can expand this out and we get a contradiction to the previous result. ♠

4.6 Proof of Theorem 4.1

Let $\{p_k/q_k\}$ and $\{B_k\}$ be as in Theorem 4.1.

Lemma 4.8 *The diameter of the largest plaid polygon in B_k tends to ∞.*

Proof: By symmetry, we can assume that the block B is one of the fundamental blocks. Let H_- and H_+ denote the two members of $\mathcal{H}$ which have capacity 2. Let V_- and V_+ denote the two members of $\mathcal{V}$ which have capacity 2. These lines intersect B in a pattern which has 4-fold dihedral symmetry. We will treat the case when H_+ lies to the left of H_- and V_+ lies to below V_-. The opposite case has a very similar treatment, and in fact follows from the first case and symmetry.

The line H_+ goes through the point $(0, y)$, where $2py \equiv 1 \bmod \omega$. We have $|y| \to \infty$ by Lemma 4.7. Hence, the separation between the lines H_+ and H_- tends to ∞ with k. By symmetry, the same goes for the separation between V_+ and V_-. In particular, the distance between H_+ and the x-axis tends to ∞. It is convenient to set $H = H_+$ and $V = V_+$.

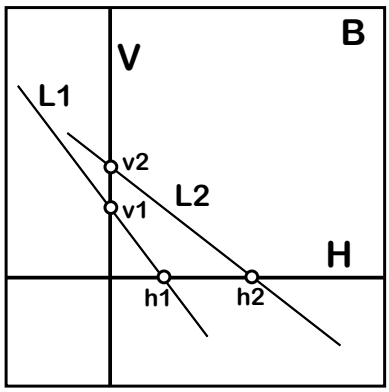

Figure 4.1: The light points on H and V.

Consider the light points v_1 and v_2 on V, as shown in Figure 4.1. If the distance between these two points tends to ∞ with k, then the plaid polygon through these points has diameter tending to ∞. So, we just have to consider the case when the distance between these points remains uniformly bounded. Since these points are symmetrically placed above and below the x-axis, both points must remain within a uniformly bounded distance of the x-axis.

One of the points, say v_1, lies on the $\mathcal{Q}$ line L_1 of mass 1. Since L_1 has slope $-Q < -1$, we know that L_1 intersects $H \cap B$ at one of the light points h_1.

In order for us to avoid finishing the proof of the theorem, the second light point h_2 on H must remain within a uniformly bounded distance of h_1. If h_2 also lies on a $\mathcal{Q}$ line, then the distance between the two $\mathcal{Q}$ lines of mass 1 remains uniformly bounded. The same reasoning as we gave for the $\mathcal{H}$ lines rules out this possibility. Thus, h_2 lies on a $\mathcal{P}$ line L_2. Since L_2 has slope $-P \in (-1, 0)$, the line L_2 intersects $V \cap B$ in the other relevant point v_2.

Consider the segments of L_1 and L_2 which have their endpoints on V and H. These two segments tend to ∞ in length and yet each endpoint of L_1 is uniformly close to an endpoint of L_2. At the same time, the slope of L_1 tends to $-1/P$ and the slope of L_2 tends to $-1/Q$. This situation is impossible. This contradiction finishes the proof. ♠

Lemma 4.9 *The number of distinct plaid polygons in B_k tends to ∞ as $k \to \infty$.*

Proof: Let M be any fixed positive integer. The side lengths of the rectangles in the grid Γ_M from the Empty Rectangle Theorem all have the form $ca_k \bmod \omega_k$, where c ranges from a uniformly bounded set. By Lemma 4.7, the minimum side length of a rectangle in Γ_M tends to ∞ with k.

By choosing k sufficiently large, we can find a collecion $R_{k,1}, ..., R_{K,N}$ of rectangles such that each $R_{k,j}$ contains a disk $D_{k,j}$ with the following two properties.

- The radius of $D_{k,j}$ tends to ∞ with k.
- $D_{k,j} \cap R_{k,i} = \emptyset$ for all $j < i$.

The idea here is that we apply the Empty Rectangle Lemma at a small scale, then at a much larger scale, and so on. In the end, we get N different rectangles which are either nested or pairwise disjoint, and in either case we can choose the scales to get the big disks.

It follows from Lemma 4.5 that each $D_{k,j}$ of these disks intersects a plaid polygon $\Gamma_{k,j}$ once k is sufficiently large. By construction, the plaid polygons $\Gamma_{k,1}, ..., \Gamma_{k,N}$ are pairwise distinct because they are separated by the rectangles. ♠

4.7 Rescaled Limits

Now we turn to the case when $\{p_k/q_k\}$ is irrationally tuned. Let $\tau \in (0,1) - \boldsymbol{Q}$ be the tuned limit. There is a unique homothety T_k such that $T_k(B_k) = [0,1]^2$. In this case, for each value of N, the rescaled grids

$$T_k(\Gamma_{k,N}) \tag{37}$$

converge (in the Hausdorff topology, say) to a grid G_M which has the following description.

- For each $k = 0, ..., M$, the grid G_M contains the horizontal lines $y = k\tau$ and $y = 1 - k\tau$. These quantities are taken mod 1. These are rescaled limits of the horizontal lines of capacity k.
- For each $k = 0, ..., M$, the grid G_M contains the vertical lines $x = k\tau$ and $x = 1 - k\tau$. These quantities are taken mod 1. These are rescaled limits of the vertical lines of capacity k.
- G_M has no other lines.

Now we consider the $\mathcal{P}$ lines and the $\mathcal{Q}$ lines. The situation here is more subtle.

$$P = \lim P_k, \qquad P_k = \frac{2p_k}{\omega_k}, \qquad Q = 2 - P. \tag{38}$$

To understand the subtlety, let's first consider the case when B_k is the first block for all k.

Lemma 4.10 *Let M be a positive odd integer. The rescaled limit $T_k(\Omega_{k,M})$ exists. It consists of the lines of slope $-P$ and $-Q$ which have y-intercept $\pm\mu\tau + \lambda$ for $\mu \in \{1, 3, 5, ..., M\}$ and $\lambda \in \boldsymbol{Z}$.*

Proof: A calculation very much like the one in the proof of Lemma 2.2 shows that, for μ odd and $\lambda \in \boldsymbol{Z}$,

$$F_{P_k}(0, \pm\mu a_k + \lambda\omega) = FP_k(0, \pm\mu) = \mp\mu/\omega_k. \tag{39}$$

Hence the $\mathcal{P}$ and $\mathcal{Q}$ lines through $(0, \pm\mu)$ have mass μ. Once k is sufficiently large, all these lines belong to $\Omega_{k,M}$ for $\mu = 1, 3, 5, .., M$. Moreover, no other points of the form $(0, y)$ satisfy $2py \equiv \pm\mu + \omega \bmod 2\omega$. ♠

Now we consider the case when $\{B_k\}$ is an arbitrary sequence of blocks. Let B_k^0 denote the first block associated to p_k/q_k and let $\Omega_{k,M}^0$ denote the corresponding set of lines. The set $T_k(\Omega_{k,M})$ differs from the set $T_k(\Omega_{k,M})$ by a vertical translation. We can take this translation to have length at most 1 because our sets are both invariant under vertical translation by 1. So, by compactness, we can pass to a subsequence and assume that $T_k(\Omega_{k,M})$ really does converge. The limit is the set of lines of slope $-P$ and $-Q$ having y-intercept $\pm\mu + \lambda + \xi$, where $\mu \in \{1, 3, 5, ..., M\}$ and $\lambda \in \boldsymbol{Z}$ and $\xi \in (0, 1)$ is the translation factor. We call ξ the *offset* of the limit.

So, if we pass to a subsequence, then the sets $\{T_k(\Gamma_{k,M})\}$ and $\{T_k(\Omega_{k,M})\}$ converge to Γ_M and Ω_M respectively. (In the final section of this chapter, we will describe a more canonical way to take rescaled limits.) We assign a capacity to the lines in Γ_M in the obvious way: If some line is the limit of lines of capacity c, it gets capacity c. Likewise, we assign a mass to the lines in Ω_M. This allows us to assign a set of light Σ_M on the lines of Γ_M.

By construction, the sets $T_k(\Sigma_{k,M})$ *practically converge* to the set Σ_M. There is one case we have to worry about. If Σ_M contains a point in the corner of $[0, 1]^2$ then it might not arise as the limit of points in $T_k(\Sigma_{k,M})$. This situation would not happen if B_k is always the first block, but it could happen in general. But we can say that every point of $\Sigma_M \cap (0, 1)^2$ is the limit of points in $T_k(\Sigma_{k,M})$. Moreover, if a light point in $\Sigma_M \cap (0, 1)^2$ is at least δ from every other point of Σ_M, then the corresponding point of $\Sigma_{k,M}$ is separated by $\delta\omega_k$ from every other light point in $\Sigma_{k,M}$.

The really interesting thing is that it seems that we can make sense of rescaled limits of individual polygons. This is beyond the scope of this paper, but we will discuss it in the last section.

4.8 The Filling Property

Now we recall a familiar fact about circle rotations. Let $\theta \in (0, 1)$ be irrational. Consider the map

$$T(x) = x + \theta \mod 1. \tag{40}$$

For any $\epsilon > 0$ there is some M such that the first M points of the orbit $\{T^j(x)\}$ is ϵ-dense. The value of M only depends on θ and ϵ and not on the starting point x. The way that M depends on θ and ϵ is subtle; it has to do with the continued fraction expansion of θ. However, we do not care about this subtlety.

Here is a consequence of the filling property. We keep the notation from the previous section.

Lemma 4.11 *Let D be a disk of radius ϵ in $[0,1]^2$. Then there is a constant M and some horizontal line L of Γ_M so that $L \cap D \cap \Sigma_M$ contains at least 2 points.*

Proof: We say that a line L *frankly intersects* a disk D if $L \cap D$ contains a point which is within radius$(D)/4$ from the center of D. If a horizontal line and a line of slope $-Q \in (-1,-2)$ both frankly intersect D, then their intersection is contained in D.

By the filling property, there is some M' such that at least 2 lines of $\Omega_{M'}$ frankly intersect D. Call these lines Q_1 and Q_2. We can take these lines to be of type $\mathcal{Q}$ and of positive sign. Also by the filling property, there is some $M > M'$ so that at least one horizontal line L having positive sign and capacity in (M', M) frankly intersects D.

We get out two points of $L \cap D \cap \Sigma_M$ by intersecting L with the two lines Q_1 and Q_2. ♠

We say a bit more about the points produced by the previous lemma.

Lemma 4.12 *Suppose that z_1 and z_2 are two points of $\Sigma_M \cap D \cap \Gamma_M$ that lie on the same horizontal line. Then at least one of the two points is distinct from every other point of $\Sigma_M \cap L$.*

Proof: Let L be the line $y = \xi_1$. Let ξ_2 be the offset of our limit. Our points have the form

$$z_j = \Big(\frac{\mu_j \tau + \xi_3}{Q}\Big), \qquad |\mu| \le M, \qquad \xi_3 = \xi_1 + \xi_2. \tag{41}$$

Given the irrationality of τ, these two points are distinct from each other, and also distinct from every other point of type Q on L.

Suppose then that z_1 and z_2 are both points of type P as well. Then we have

$$|z_1 - z_2| = \frac{c_1}{P} = \frac{c_2}{Q}, \qquad c_1, c_2 \in \boldsymbol{Z}. \tag{42}$$

This contradicts the fact that P/Q is irrational. ♠

4.9 Proof of Theorem 4.2

We will work with the rescaled limit and then, at the end, interpret what our result says.

The Empty Rectangle Lemma applies to the grid Γ_M By varying M and applying the Empty Rectangle Lemma N times, we can find N rectangles in $[0,1]^2$, say $R_1, ..., R_N$ such that each R_j contains a disk D which is disjoint from R_i for $j < i$. The filling property lets us take N as large as we like.

By the work in the previous section, each disk D_j will contain a light point z_j. which is distinct from all other light points on the same horizontal line. Let 2δ be the minimum separation between z_j and any other light point. The minimum is taken over all $j = 1, ..., N$. By making δ smaller, if necessary, we can arrange that every disk of radius $1/2N$ contains the kind of light point which is separated from its horizontal neighbors by at least 2δ.

Now let us see what this says about the picture in the block B_k. Once k is sufficiently large, we can find rectangles $R_{k,1}, ..., R_{k,N}$ which contain disks $D_{k,1}, ..., D_{k,N}$ having the following propertyes.

- $D_{k,j}$ is disjoint from $R_{k,i}$ if $j < i$.
- $D_{k,j}$ contains a light point $z_{k,j}$ which is separated from all other light points on the same horizontal line by at least $\delta\omega_k$.

Let $\Gamma_{k,j}$ denote the plaid polygon that intersects the horizontal unit segment containing z_j. Since $\Gamma_{k,j}$ is a closed loop, it must intersect the horizontal line containing $z_{k,j}$ in a second light point. Hence $\Gamma_{k,j}$ has x-diameter at least $\delta\omega_k$. By construction, the polygons $\Gamma_{k,j}$ and $\Gamma_{k,i}$ lie in different components of $B_k - \partial R_{k,j}$ for $j < i$. Hence, these polygons are all distinct.

At the same time, choose any tile center $c \in B_k$. Let Δ be the disk of radius ω_k/N about c. Then $T_k(\Delta)$ contains a disk of radius $1/2N$ for k large. Hence $T_k(\Delta)$ contains a light point that is separated from its horizontal neighbors by at least 2δ. But then the inverse image of this point is a light point in Δ that is is separated from all the other light points on the same horizontal line by at least $\delta\omega_k$. Hence, c is within ω_k/N of some plaid polygon having diameter at least $\delta\omega_n$.

This completes the proof of Theorem 4.2.

5 The Action on Particles

5.1 Overview

Let $\mathcal{C}$ denote the set of centers of square tiles. Let Ξ be the classifying map from §3.2. To prove the Isomorphism Theorem we need to study the image $\Xi(\mathcal{C})$. One could say that our proof of the Isomorphism Theorem has a product structure to it. In this chapter, we underStand what the classifying map does to those subsets of $\mathcal{C}$ corresponding to the particles discussed in §2.6. We won't analyze where these subsets get mapped in, but we will be able to describe their geometry. That is, we will understand their images up to translation.

In the next chapter, we understand where precisely the classifying map takes certain elements of $\mathcal{C}$ which correspond to specially chosen instances of the particles. This information allows us to anchor the geometric picture obtained in this chapter, so to speak. In §7 we will put the two pieces of information together and finish the proof of the Isomorphism Theorem. In our analysis, we will work with the west and south edges. It turns out that this is all we need.

We fix an even rational $p/q \in (0,1)$. Let $\omega = p+q$. Let $z_0, ..., z_{n-1}$ denote the portion of a particle in which z_j does not change type. There are three cases.

- If the particle is vertical, then $n = \omega$.
- If the particle is horizontal and the points have type P then z_0 is contained in the left edge of the boundary and $n = 2p$.
- If the particle is horizontal and the points have type Q then z_0 is contained in the right edge of the boundary and $n = 2q$.

Let $c_0, ..., c_{n-1}$ denote the set of centers of unit squares in the block such that z_i belongs to the west (respectively south) edge of the square centered at c_i provided that the particle is vertical (respectively horizontal). We are interested in the image

$$Z = \bigcup_{i=0}^{n-1} \Xi(c_j) \subset X_P. \tag{43}$$

The goal of this chapter is to understand the set Z.

5.2 The Vertical Case

For our analysis, we will drop off the first coordinate of $\{P\} \times X_P$ and work in $\boldsymbol{R}^3$. Recall that X_P has coordinates (T, U_1, U_2), with (U_1, U_2) being the fiber.

Lemma 5.1 *Suppose that Z corresponds to a vertical particle of type P. Then Z is contained in a single fiber and lies in a line $U_1 = \text{const}$.*

Proof: Let $c = c_j$ and $c' = c_{j+1}$. We will suppose that the particle is of type P. This means that

$$c' = c + (a\omega, 1), \qquad 2ap \equiv -1 \mod \omega. \tag{44}$$

According to Equation 17 we have

$$\Psi(c') - \Psi(c) = (2Pa\omega, 2Pa\omega - P, 2Pa\omega + P) \mod \Lambda_P. \tag{45}$$

Note that $Pa\omega \in \boldsymbol{Z}$. Subtracting off $Pa\omega$ times $(2, 2+P, 2+P)$, we get

$$.\Psi(c') - \Psi(c) = (0, P(-1 - Pa\omega), P(1 - Pa\omega)) \mod \Lambda_P. \tag{46}$$

Note that $-1 - Pa\omega = K\omega$ for some $K \in \boldsymbol{Z}$. Hence $K\omega P = 2Kp \in 2\boldsymbol{Z}$. Hence the U_1 coordinate in Equation 46 vanishes. ♠

The same argument, or an appeal to symmetry, yields the following.

Lemma 5.2 *Suppose that Z corresponds to a vertical particle of type Q. Then Z is contained in a single fiber and lies in a line $U_2 = \text{const}$.*

5.3 A Revealing Picture

Before we deal with the horizontal particles, we draw a picture of Z in the (T, U_j) plane. Up to vertical translation, the images all look the same. They are all contained in parallelograms whose sides have slope 0 and 1. These parallelograms look the same for both $j = 1$ and $j = 2$, up to translations. The left hand side pertains to the type P portion of the particle and the right hand side pertains to the type Q portion. The middle picture shows how they two pieces fit together, and also labels some distances in the picture.

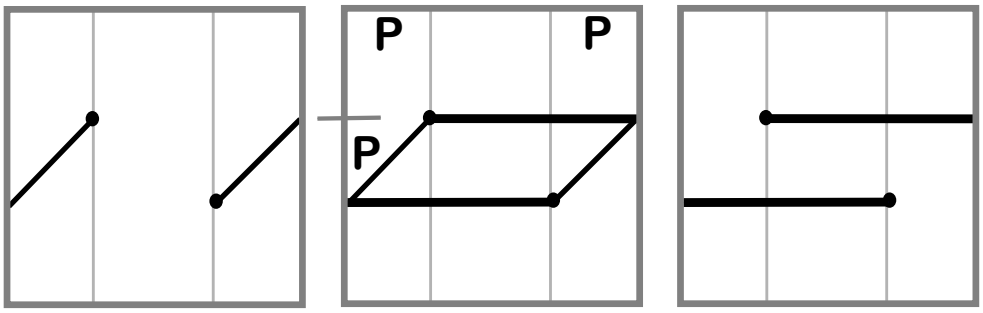

Figure 5.1: A typical set Z drawn in the (T, U_j) plane.

It is worth pointing out that the parallelogram in the middle figure is not embedded. It has a double point which appears when the left edge of the picture is identified to the right edge by the map $(-1, y) \to (1, y + P)$. This double point is the image of the midpoint of one horizontal edge that is right in the middle of a block. All the particles pass twice through a double point like this.

5.4 The Horizontal Case: Type P

Lemma 5.3 *Suppose that Z corresponds to a horizontal particle of type P. Then Z is contained in a single line segment S parallel to $(1, 1, 1)$ which does not intersect and of the fibers over $T \in (-1 + P, P - 1)$.*

Proof: To simplify the argument, we claim that the result is true for one particle $z_0, ..., z_{2p-1}$ of this type if and only if it is true for another particle $z'_0, ..., z'_{2p-1}$ of this type. Let $c'_0, ..., c'_{2p-1}$ and Z' be the objects associated to this other particle. Since both z_1 and z' belong to the left edge of some block, we have

$$z'_j = z_j + (k_1(p+1), k_2), \quad c'_j = c_j + (k_1(p+1), k_2), \qquad \forall j. \tag{47}$$

$$\Xi(c'_j) - \Xi(c_j) = (2Pk_1\omega, \alpha_1, \alpha_2 = (0, \beta_1, \beta_2) \mod \Lambda. \tag{48}$$

This works because $2Pk_1\omega$ is an even integer. Here $\alpha_1, \alpha_2, \beta_1, \beta_2$ are independent of j. Thus Z' is obtained from Z by applying some fiber-preserving transformation. This establishes our claim.

In view of our claim, it suffices to work with the particle

$$z_k = (ka\omega + k/P, 0), \qquad k = 0, ..., 2p-1. \tag{49}$$

As usual, $2ap \equiv -1 \bmod P$.

To simplify our calculation, we work with the points $\widehat{c}_0, ..., \widehat{c}_{2p-1}$, where $\widehat{c}_j$ lies on the midpoint of the horizontal segment containing z_j. We have $\widehat{c}_0 = c_0 - (0, 1/2)$. Furthermore, we work with the map $\widehat{\Xi} = \Xi - (1, 0, 0)$. We have

$$\widehat{\Xi}(x, 0) = (2Px, 2Px, 2Px). \tag{50}$$

Let $\widehat{Z}$ be the modified version of Z. Using the formulas in §3.8, we see that the statement of this lemma is equivalent to the statement that $\widehat{Z}$ is contained in a line segment parallel to $(1, 1, 1)$ and is contained in the union of fibers lying over $[-P, P]$.

Note that $2P(k/P)$ is always an even integer. Hence $\widehat{\Xi}(z_j) = (0, 0, 0)$. The points $\widehat{c}_j$ and z_j are on the same unit segment and differ by at most $1/2$ units. Hence $\widehat{\Xi}(\widehat{c}_j)$ lies on the segment joining $(-P, -P, -P)$ to (P, P, P). ♠

5.5 A Technical Result

Recall that $[x]_2$ is the value of x mod $2\boldsymbol{Z}$ that lies in $[-2, 2)$. Recall also that $P + Q = 2$. Here we prove a technical result.

Lemma 5.4 *Let $m, k \in \boldsymbol{Z}$ and let $c = m + 1/2$. If $k/Q \in [m + 1/Q, m + 1]$ then $[2Pc + 1]_2 \in [-1 + P, 1 - P]$.*

Proof: The conditions imply that $2k \in [2Qm + 2, 2Qm + 2Q]$. Hence, there is another even integer integer

$$e \in [-2Qm - (2Q - 2), -2Qm] = [-2Qm - (2 - 2P), -2Qm].$$

We have

$$2Pc + 1 = 2Pm + P + 1 \equiv -2Qm - (1 - P) \bmod 2\boldsymbol{Z}.$$

But then

$$[2Pc + 1]_2 = -2Qm - (1 - P) - e \in [-1 + P, 1 - P].$$

This completes the proof. ♠

5.6 The Horizontal Case: Type Q

Lemma 5.5 *Suppose that Z corresponds to a horizontal particle of type Q. Then Z is contained in a single line segment S, parallel to $(1,0,0)$, with the following structure.*

- *S intersects the fibers over $[-1,-1+P) \cup [P_1,1]$ once.*
- *S intersects the fibers over $[-1+P, 1-P]$ twice.*

Proof: By the same kind of argument given in the previous result, it suffices to work with the dark particle $z_0, ..., z_{2q-1}$, where

$$z_k = (ka\omega - k/Q, 0). \tag{51}$$

Likewise, we work with the points $\widehat{c}_0, ..., \widehat{c}_{2q-1}$. This time we will work with the map Ξ. There are 2 cases:

Case 1: Suppose that $c = m+1/2$ and $z_k \in [m+1/Q, m+1]$ for some integer m. By Lemma 5.4, we can say that $\Xi(\widehat{c}_k)$ lies in a fiber over $[-1+P, 1-P]$. In this case there are 2 points of type Q in the interval containing $\widehat{c}_k$ and so

$$\widehat{c}_{k+1} = \widehat{c}_k + (a\omega, 0). \tag{52}$$

Since $2Pa\omega = 4ap$, we have

$$\Xi(\widehat{c}_{k+1}) - \Xi(\widehat{c}_k) = (4ap, 4ap, 4ap) = (0, -2Pap, -2Pap) \mod \Lambda_P.$$

But $-2Pap \equiv P \bmod 2\boldsymbol{Z}$. Hence

$$\Xi(\widehat{c}_{k+1}) - \Xi(\widehat{c}_k) = (0, P, P) \mod \Lambda_P. \tag{53}$$

Case 2: Now suppose that $c = m + 1/2$ and $z_1 \in (m, m + 1/Q)$. (The case $z_k = m$ does not occur; it would be the point z_{2q}.) In this case, we have

$$\widehat{c}_{k+1} = \widehat{c}_k + (a\omega - 1, 0). \tag{54}$$

It follows from Equation 53 that

$$\Xi(\widehat{c}_{k+1}) - \Xi(\widehat{c}_k) = (-2P, P, P) = (2 - 2P, 0, 0) \mod \Lambda_P. \tag{55}$$

Let $Z_k = \Xi(\widehat{c}_j)$. We have $Z_0 = (1, P/2, P/2)$. In Figure 5.1 this point would be all the way on the right. Let L be the line segment from the lemma which contains Z_0. If we forget the identifications on $[-1,1]^3$, then L becomes 2 line segments, the *upper half* contains Z_0 and the *lower half* does not. At the same time, we divide $[-1,1]^3$ into 3 *zones*, depending on where T falls in the partition $[-1, -1+P, 1-P, 1]$. The vertical line segments in Figure 5.1 demarkate these zones. We say that a point is *left lower* if it lies in the left zone and on the lower half of L. We give similar names to the other possibilities. The two cases above tell us the following.

- If Z_k is left lower, then Z_{k+1} is left lower or middle lower.
- If Z_k is middle lower then Z_{k+1} is middle upper.
- If Z_k is middle upper then Z_{k+1} is right upper or left lower.
- If Z_k is right upper then Z_{k+1} is left lower or middle lower.

In the last two cases, we use the action of Λ in case the addition of $2-P$ to the T coordinate causes the value to increase beyond 1. Since $Z_0 \in L$, we have $Z_k \in L$ for all L. ♠

For later use, we want to extract something more out of the proof of Lemma 5.5. The following result is a consequence of our argument given in the proof of Lemma 5.5.

Lemma 5.6 *Suppose that z_1 and z_2 are two intersection points contained in the same south edge of some unit square centered at the point c. Suppose that z_1 lies to the left of z_2. Then there are other instances z_1' and z_2' of z_1 and z_2 respectively so that*

- *$\Xi(c_1)$ lies in the fiber over $T=1$ and $\Xi(c_1)$ and $\Xi(c)$ are joined by a segment in $[-1,1]^3$ parallel to $(1,0,0)$.*
- *$\Xi(c_2)$ lies in the fiber over $T=-1$ and $\Xi(c_2)$ and $\Xi(c)$ are joined by a segment in $[-1,1]^3$ parallel to $(1,0,0)$.*

Here $c_j \in \mathcal{C}$ is a point such that the south edge of the square containing z_j' is contained in c_j.

6 The Images of Symmetric Points

6.1 Overview

We fix an even rational p/q as usual. Let $\omega = p + q$. Let $z_1, ..., z_n$ be a particle and let $c_1, ..., c_n$ be the edges corresponding to these points. If $\{z_i\}$ is a vertical (respectively horizontal) particle, then c_i is the center of the unit square whose west (respectively south) edge contains z_i.

In the vertical case, we call z_i a *symmetric instance* of the particle if c_i is centered on the horizontal midline of the block. That is

$$c_i = (x + 1/2, k\omega + \omega/2), \qquad k, x \in \boldsymbol{Z}. \tag{56}$$

In the horizontal case, we call z_i a symmetric instance if c_i is centered on the vertical midline of the block. That is,

$$c_i = (k\omega + \omega/2, y + 1/2), \qquad k, y \in \boldsymbol{Z}. \tag{57}$$

Every vertical particle has one symmetric instance, and every horizontal particle has two symmetric instances - one as type P and one as type Q. In the horizontal case, the symmetric instances of the particle correspond to the double point in Figure 5.1.

Let $\mathcal{V}_k$ denote the subset of points c in Equation 56 such that the west edge of the square centered at c has k light points of type P in them. Likewise, let $\mathcal{H}_k$ denote the subset of points c in Equation 57 such that the soth edge of the square centered at c has k light points of type P in them. These sets are empty unless $k = 0, 1$.

In this chapter, we will $\Xi(\mathcal{V}_k)$ and $\Xi(\mathcal{H}_k)$ for $k = 0, 1$. (By symmetry, these sets are the same if we use type Q particles instead of type P particles.) Once we have this information, we will combine it with what we did in the last chapter to finish the proof of the Isomorphism Theorem.

For our analysis, it is awkward to work directly with the centers of the squares. It is better to work with the centers of the edges which contain the particles. We define

$$\mathcal{V}'_k = \mathcal{V}_k - (1/2, 0), \qquad \mathcal{H}'_k = \mathcal{H}_k - (0, 1/2). \tag{58}$$

In each case, we will analyze what Ξ does to these sets, and then we will make the tedious but routine translation back to the original sets of interest to us.

6.2 Good Pairs

Suppose that a_1, a_2 are real numbers. We say that (a_1, a_2) is a *good pair* if none of the numbers $a_1, a_2, a_1 - a_2$ is an integer and

$$[a_1]_2\ [a_2]_2 > 0, \qquad ||a_1]_2| < |[a_2]_2|. \tag{59}$$

These are exactly the conditions we used in the grid description of the plaid model. Figure 6.1 shows the set of good pairs (a_1, a_2) in the square $[-1, 1]^2$.

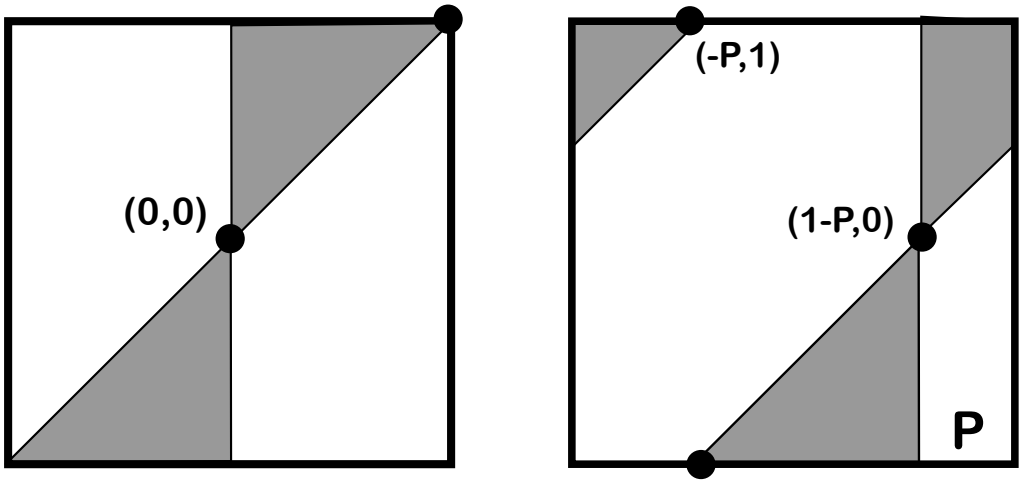

Figure 6.2: The set of good pairs

Now we prove a technical lemma about good pairs which will be helpful in the horizontal case. Define

$$b_1 = a_1 - a_2, \qquad b_2 = a_1 - 1. \tag{60}$$

Lemma 6.1 *(a_1, a_2) is a good pair if and only if (b_1, b_2) is a good pair.*

Proof: Since the affine transformation $T(x, y) = (x - y, x - 1)$ preserves $\boldsymbol{Z}^2$, the pair (a_1, a_2) satisfies the non-integrality condition if and only if the pair (b_1, b_2) does. If this lemma is true for the inputs (a_1, a_2) it is also true for the inputs $(a_1 + 2k_1, a_2 + 2k_2)$ for any integers k_1, k_2. For this reason, it suffices to consider the case when $a_1, a_2 \in (-1, 1)$. From here, an easy case-by-case analysis finishes the proof. For instance, if $0 < a_1 < a_2$ then $0 > b_1 > b_2$. The other cases are similar. ♠

6.3 The Vertical Case

We drop the first coordinate and work in $[-1,1]^3$ with the (T,U_1,U_2) coordinates. We define the *diagonal* ΔX of X to be the set where $U_1 = U_2$.

Lemma 6.2 *Let $G' \subset \Delta X$ be the set such that (T,U_k) is a good pair. Then $\Xi(\mathcal{V}'_0) \subset \Delta X - G'$ and $\Xi(\mathcal{V}'_1) \subset G'$ and*

Proof: Let $c \in \mathcal{V}'_k$. It follows from Lemma 3.5 (or direct calculation) that $\Xi(c) \in \Delta X$. The corresponding intersection point $z = (x,y)$ lies on a line of slope $-P$ which has an integer y-intercept. Hence

$$y = \omega/2 - [Px + \omega/2]_1.$$

Here $[t]_1$ denotes the number in $[-1/2, 1/2)$ that differs from t by an integer. Since $[t]_1 = [2t]_2/2$, we get

$$y = \omega/2 - \frac{1}{2}[2Px + \omega]_2 =^* \omega/2 - \frac{1}{2}[2Px+1]_2 = \omega/2 - T(c)/2. \tag{61}$$

The starred equality uses the fact that $\omega - 1 \in 2\boldsymbol{Z}$. Define

$$z' = (x,y) + T(c)/2. \tag{62}$$

Reflection in the horizontal midline of the block swaps z and z'. By symmetry, z is a light point of type P if and only if z' is a light point of type Q. We will work with z'. We compute

$$F_V(z') = [2Px]_2 = [T(c)+1]_2. \tag{63}$$

Next, we compute

$$F_Q(z') = [Py + PQx + 1]_2 = [P\omega/2 + PT(c)/2 + PQx + 1]_2.$$

Looking at the equations from §3.8, we recognize this last expression as $[U_2(c)+1]_2$. Since $U_2(c) = U_1(c)$, we have

$$F_Q(z') = [U_1(c)+1]_2. \tag{64}$$

From Equations 63 and 64 we see that $F_V(z')$ and $F_Q(z')$ have the same sign if and only if $T(c)$ and $U_1(c)$ have the same sign and $|F_Q(z')| < |F_V(z')|$ iff $|T(c)| < |U(c)|$. Hence $\Xi(c) \in \Delta X - G'$ if $k = 0$ and $\Xi(c) \subset G'$ if $k = 1$ ♠

6.4 The Vertical Case Translated

Now we translate the picture so that we are working with $\Xi(\mathcal{V}_k)$ rather than $\Xi(\mathcal{V}'_k)$. Let

$$\rho(x, y) = (x + 1/2, y). \tag{65}$$

We have

$$\rho(\mathcal{V}'_k) = \mathcal{V}_k. \tag{66}$$

A direct calculation shows that

$$\Psi \circ \Xi = \Xi \circ \rho, \qquad \Psi(x_1, x_2, x_3) = (x_1, x_2, x_3) + (P, P, P). \tag{67}$$

Hence

$$\Xi(\mathcal{V}_k) = \Xi(\mathcal{V}'_k) + (P, P, P) \qquad \text{mod } \Lambda_P. \tag{68}$$

Note that $\Psi(\Delta X) = \Delta X$. We draw G' and $G = \Psi(G)$ side by side in Figure 6.2.

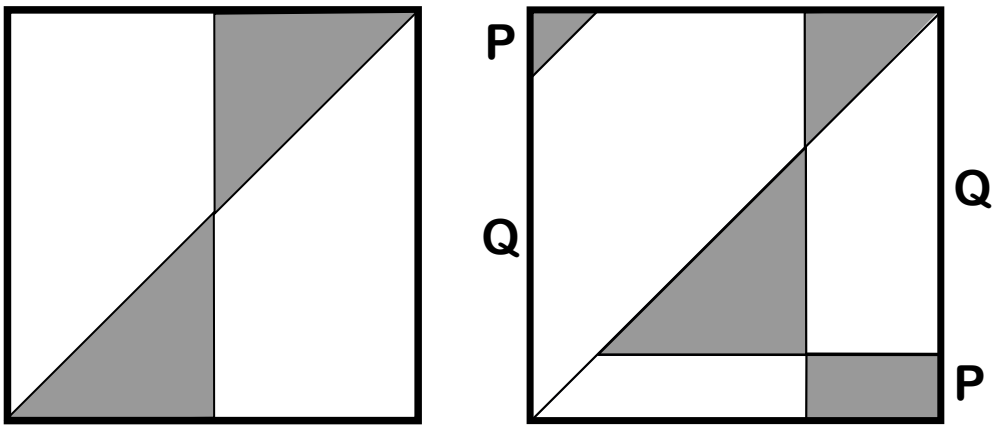

Figure 6.2: G' on the left and G on the right.

Combining Lemma 6.2 with the description in this section, we get the following result.

Lemma 6.3 *Let $G = \Psi(G')$. Then $\Xi(\mathcal{V}_0) \subset \Delta X - G$ and $\Xi(\mathcal{V}_1) \subset G$ and*

Remark: The left and right sides of G really do match up, because these sides are identified mod Λ_P. In the picture, the point $(-1, y)$ matches with $(1, y + P)$ if $x < 1 - P$ and otherwise with $(1, y - Q)$.

6.5 The Horizontal Case

We will get a nicer answer if we use the alternate map

$$\Xi' = \Psi_0^{-1} \circ \Xi, \qquad \Psi_0(T, U_1, U_2) = (T, U_1 - P/2 - 1, U_2 - P/2). \tag{69}$$

Ξ' differs from Ξ only by a fiber-preserving translation. We define

$$(T', U_1', U_2') = \Psi_0^{-1}(T, U_1, U_2). \tag{70}$$

Let U denote the fiber over $T = -1$.

Lemma 6.4 *Let G' denote the set in U such that (U_1, U_2) is a good pair. Then $\Xi'(\mathcal{H}_0') \subset U - G'$ and $\Xi'(\mathcal{H}_1') \subset G'$.*

Proof: Let $c = (x, y)$ be some point of $\mathcal{H}_\parallel'$. Using the fact that $x = 2k\omega + \omega/2$, we compute

$$F_P(c) = F_Q(c) = [Py + PQx + 1]_2, \qquad F_H(c) = [2Py]_2. \tag{71}$$

Let a_1 and a_2 be these two numbers. Next, we compute

$$U_1' = [-Py + PQx + 1]_2, \qquad U_2' = [Py + PQx]_2. \tag{72}$$

Let b_1 and b_2 be these two numbers. The numbers a_1, a_2, b_1, b_2 satisfy the hypotheses of Lemma 6.1. Lemma 6.1 now finishes this proof. ♠

6.6 The Horizontal Case Translated

Define

$$\rho(x, y) = (x, y + 1/2). \tag{73}$$

$$\Psi_1(T, U_1.U_2) = (T, U_1 - P/2, U_1 + P/2) \tag{74}$$

We have

$$\Xi \circ \rho = \rho \circ \Psi_1, \qquad \rho(\mathcal{H}_k') = \mathcal{H}_k. \tag{75}$$

Putting all this together, we have

$$\Xi(\mathcal{H}_k) = \Psi_1(\Xi(\mathcal{H}_k')) = \Psi_1 \Psi_0 \Xi'(\mathcal{H}_k'). \tag{76}$$

Note that

$$\Psi_1 \Psi_0(T, U_1, U_2) = (T, U_1 + (1 - P), U_2). \tag{77}$$

So, $\Xi(\mathcal{H}_k)$ is obtained from $\Xi(\mathcal{H}_k')$ by applying a horizontal translation of the fiber by $(1 - P, 0)$. Figure 6.3 shows the sets G' and G.

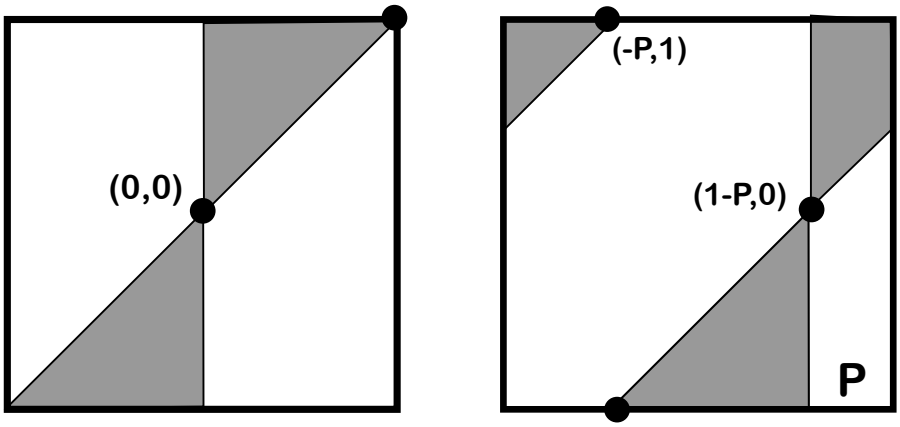

Figure 6.3: G' on the left and G on the right.

Define

$$\Psi(U, T_1, T_2) = (U, T_1 + 1 - P, T_2). \tag{78}$$

Lemma 6.5 *Let $G = \Psi(G')$. Then $\Xi(\mathcal{H}_0) \subset U - G$ and $\Xi(\mathcal{H}_1) \subset G$.*

7 The Isomorphism Theorem

7.1 Nine Sets of Centers

We want to prove that the grid light set and the tile light set coincide for any square tile, and edge of the square, and any parameter. Using the fact that reflections in the horizontal and vertical midlines of the fundamental domain are symmetries of both the grid light set and the tile light set, it suffices to prove our result for the west and south edges of the squares. We fix some even rational parameter p/q.

Recall that $\mathcal{C}$ is the set of centers of the square tiles. For each symbol $A \in \{S, W\}$ and each symbol $B \in \{P, Q\}$ and each integer $k = 0, 1, 2, ...$ we define $\mathcal{S}(A, B, k)$ to be the set $c \in \mathcal{C}$ such that the grid description assigns k light points of type B to the A edge of the square centered at c.

Here are some easy observations.

- Since the $\mathcal{P}$ lines have slope $-P \in (-1, 0)$, and intersect the y-axis at integer points, $\mathcal{S}(H, P, k) = \emptyset$ for $k > 1$.
- Since the $\mathcal{Q}$ lines have slope $-Q \in (-2, -1)$ and intersect the y-axis at integer points, $\mathcal{S}(H, P, k) = \emptyset$ for $k > 2$.
- Since the $\mathcal{P}$ and $\mathcal{Q}$ lines intersect the y axis at integer points, the light points of either type on a $\mathcal{V}$ line are spaced integer distances apart. Hence $\mathcal{S}(V, B, k) = \emptyset$ for $B \in \{P, Q\}$ and $k > 1$.

So, there are just 9 nontrivial sets.

As we have mentioned already, our strategy for understanding the locations of these sets in the classifying space is to observe that each one of them contains one of the images we considered in §6:

$$\mathcal{V}_k \subset \mathcal{S}(P, V, k) \cap \mathcal{S}(Q, V, k), \qquad k = 0, 1. \tag{79}$$

$$\mathcal{H}_0 \subset \mathcal{S}(P, V, 0) \cap \mathcal{S}(Q, V, 0), \quad \mathcal{H}_1 \subset \mathcal{S}(P, H, 1) \cap \bigcup_{k=1}^{2} \mathcal{S}(Q, H, k). \tag{80}$$

Each of the sets considered in §6 contains the image of a west or south edge containing at least one instance of each particle. Using the results from particles obtained in §5 we will be able to pin down the images of the 9 sets exactly.

7.2 The West Edges

We first describe a certain subset $\Sigma(W, Q, 1) \subset X$, fiber by fiber.

- When the fiber lies over $T \in (-1 + P, P)$, the set $\Sigma(W, Q, 1)$ consists of all points in the fiber lying on horizontal lines through the square labeled W.
- Otherwise, $\Sigma(W, Q, 1)$ consists of all points in the fiber lying on horizontal lines which avoid W.

Figure 7.1 shows a picture of the two cases.

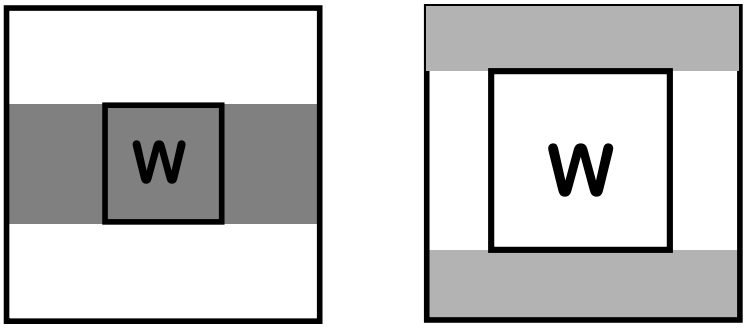

Figure 7.1: The set $\Sigma(W, Q, 1)$ intersecting a fiber.

The left hand side of Figure 7.2 gives a further guide to $\Sigma(W, Q, 1)$. We have translated the square torus so that the W square is at the center of the picture, but in most fibers the picture will not be centered this way.

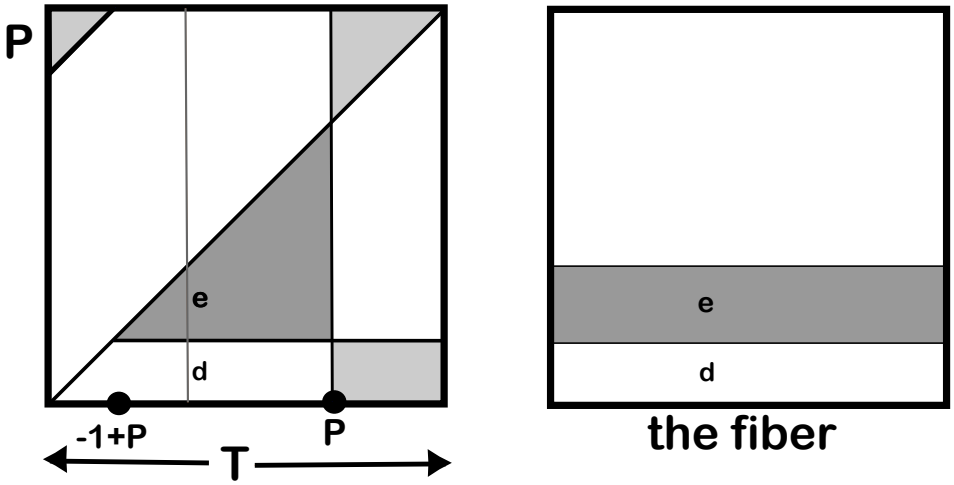

Figure 7.2: A guide to understanding $\Sigma(W, Q, 1)$.

The picture is drawn when $P \approx 1/3$ but the set is the same for all choices of P, up to translation (on the torus). The way the picture works is that you draw a vertical line T units over from the left. You see how this vertical line intersects the shaded region in the picture. Then you construct a horizontal strip in the fiber $[-1,1]$ so that the vertical line intersects the strip the same way.

The set is not defined in the fiber $T = P$. However, as discussed in §3.5, the classifing map does not map any points of $\mathcal{C}$ into this transitional fiber. Next, define

- $\Sigma(W,Q,0) = X - \Sigma(W,Q,1)$.
- $\Sigma(W,P,k) = \Xi(\Sigma(W,P,k)$ for $k = 0,1$.

Lemma 7.1 *Ξ maps $\mathcal{S}(V,Q,k)$ into $\Sigma(V,Q,k)$ for $k = 0,1$.*

Proof: Comparing Figure 7.2 wish our description of the set $G \subset \Delta X$ given in §6.4 and shown on the right hand side of Figure 6.2, we see that $\Sigma(V,Q,1)$ has the following description. We take the union of the lines parallel to $(0,1,0)$ through all the points of G and intersect them with $[-1,1]^3$. At the same time we define $\Sigma(V,Q,0)$ has the same description, using $\Delta X - G$ in place of G. This lemma now follows from Lemma 5.2, Lemma 6.3 and Equation 79. ♠

Lemma 7.2 *Ξ maps $\mathcal{S}(V,P,k)$ into $\Sigma(V,P,k)$ for $k = 0,1$.*

Proof: This follows from Lemma 7.1, the definition of $\Sigma(W,P,k)$, and the symmetry established in Lemma 2.3 and Lemma 3.5. ♠

Let $S_1 \Delta S_2$ denote the symmetric difference of the sets, namely

$$S_1 \Delta S_2 = (S_1 - S_2) \cup (S_2 - S_2).$$

Looking at the picture fiber by fiber, we see that

$$\Sigma(W,P,1)\Delta\Sigma(W,Q,1) = X_{WS} \cup X_{WE} \cup X_{WN}. \tag{81}$$

Here X_{WS}, etc., are the sets which comprise the partition of the classifying space X. Let $c \in \mathcal{C}$ be a center of a square tile. Let w be the west edge of the

tile centered at c. Suppose that the grid model assigns 0 or 2 light point to w. Then either $c \in \mathcal{S}(V, B, 0)$ for both choices of $B \in \{P, Q\}$ or for neither choice. But then

$$\Xi(c) \notin \Sigma(V, P, 1)\Delta\Sigma(V, Q, 1).$$

Hence $\Xi(c) \notin X_{WS} \cup X_{WE} \cup X_{WN}$. But then the tile description assigns a tile to c whose connector does not involve the w.

Suppose on the other hand that w has one light point. Then

$$\Xi(c) \in \Sigma(V, P, 1)\Delta\Sigma(V, Q, 1).$$

Hence $\Xi(c) \in X_{WS} \cup X_{WE} \cup X_{WN}$, and the tile description assigns a tile to c whose connector does involve w. This completes the proof of the Isomorphism Theorem for the west edges. Again, the case of the east edges follows from symmetry.

Remark: In writing the equations above, we have been a bit sloppy about the boundaries of our sets, but the same analysis as given in §3.5 shows that the image of $\mathcal{C}$ avoids the boundaries of the relevant sets.

7.3 The South Edges

Now we define sets $\Sigma(S, P, k)$ for $k = 0, 1$ and $\Sigma(S, Q, k)$ for $k = 0, 1, 2$. Again, we give a fiberwise description of these sets. The picture we show is a diagram which requires some interpretation. We will show the picture first and then give the interpretation.

The left hand side of Figure 7.2 shows the labeling we use for fibers lying above points $T \in [1-P, -1+P]$ and the right hand picture shows the labeing we use for the fibers lying over the remaining points. Notice that this is the same dichotomy that appears in Lemmas 5.3 and 5.5, which deal with the images of horizontal particles of type P and Q respectively.

We have drawn the picture with the square labeled S in the center of the torus, but in each fiber we mean to construct these sets based on the true location of S. The diagonal lines are such that they bisect the edges of the square fundamental domain.

For each $B \in \{P, Q\}$ we define $\Sigma(S, B, 1)$ to be the union, taken over all fibers, of the regions which have a B label in them. The exception is the label Q2, which does not count as an instance of the Q label.

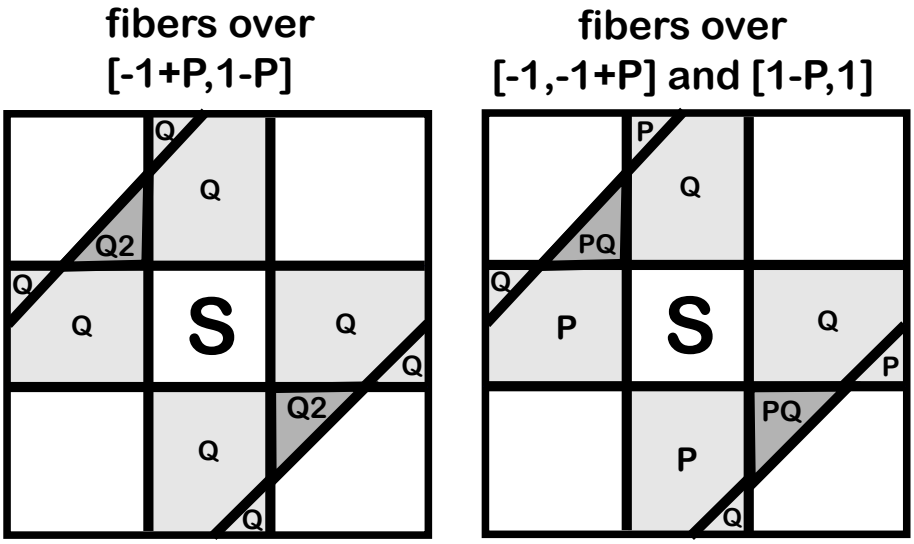

Figure 7.2: Guide to the sets

Notice also that $\Sigma(S,P,1) \cap \Sigma(S,Q,1)$ is the union of all the regions labeled PQ. Finally we define $\Sigma(S,Q,2)$ as the union of the regions labeled Q2. We define $\Sigma(S,P,0)$ each to be the union of the unlabeled pieces - i.e., the complement of the sets defined by the labels.

Below we will prove the following result.

Lemma 7.3 *For each $B \in \{P,Q\}$ and each relevant $k \in \{0,1,2\}$, the set $\mathcal{S}(H,B,k)$ is mapped into $\Sigma(H,B,k)$ by Ξ.*

Assume Lemma 7.3 for the moment. By inspecting each of the two types of fibers, we see the following relations

$$\Sigma(S,P,1)\Delta\Sigma(S,Q,1) = X_{SE} \cup X_{SW} \cup X_{SN}. \tag{82}$$

$$\Sigma(S,Q,k) \cap (X_{SE} \cup X_{SW} \cup X_{SN}) = \emptyset, \qquad k = 0,2. \tag{83}$$

Assuming Lemma 7.3 and the above two relations, the rest of the proof of the Isomorphism Theorem for the south edges is exactly as it was for the west edges.

The rest of the section is devoted to proving Lemma 7.3. We will break this result up into several smaller ones.

Lemma 7.4 *Ξ maps $\mathcal{S}(H,P,k)$ into $\Sigma(H,P,k)$ for $k = 0,1$.*

Proof: Looking at Equation 20 we see that as $T \to -1$, the square labeled S shrinks to the point $(1-P, -1)$. Therefore, the right hand side of Figure 6.3, with the shaded region labeled PQ, shows what our sets $\Sigma(H, P, k)$ look like above the fiber $T = -1$. We call these intersections $\Sigma_0(H, P, k)$. For convenience, we repeat the picture below.

Let $\Sigma_t(H, P, k)$ be the intersection of $\Sigma(H, P, k)$ with the fiber over $-1+t$. We imagine $t \in [-P, P]$ as a parameter. We know the picture at $t = 0$ and we want to understand what happens as t varies.

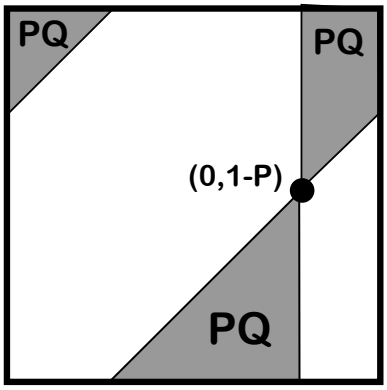

Figure 7.3: The set $\Sigma_0(H, P, 1)$ is shaded.

Looking at the right hand side of Figure 7.2, we see $\Sigma_t(P, H, k)$ is just a translate of $\Sigma_0(P, H, k)$. Here we have included the portion of the right hand side of Figure 7.2 which just shows the regions with the P labels.

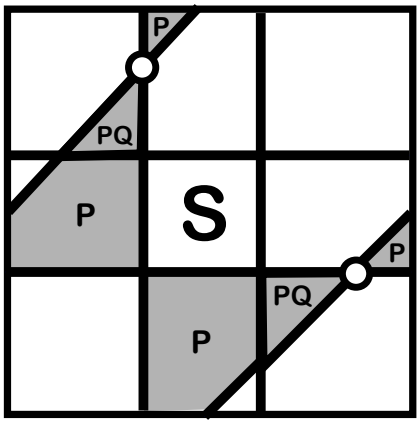

Figure 7.4: $\Sigma(H, P, 1)$ over a fiber in $[-1+P, 1] \cup [1-P, 1]$.

Call the marked points in Figure 7.4 the *apices* of the fiber. Each apex lies on a vertical geodesic extending a vertical edge of the square S and is half way around the fiber from the center of this edge. From this description, and from Equations 20 and 22 (and, to be honest, from computer drawings) we see that the apices move with speed 1 along lines of slope 1 as a function of t. In otherwise, we obtain $\Sigma_t(H,P,k)$ from $\Sigma_0(H,P,k)$ by translating along the vector (t,t,t).

Combining this information with Lemma 5.3 and Lemma 6.5, we get the conclusion of this lemma. ♠

Lemma 7.5 *Let $c \in \mathcal{S}(H,Q,k)$ for some k and suppose that $\Xi(c)$ is contained in a fiber over $T \in [-1,-1+P]$. Then $\Xi(c) \in \mathcal{S}(H,Q,k)$.*

Proof: The proof is similar to what we did in Lemma 7.5. For $t \in [-1,-1+P]$ the set $\Sigma_t(H,Q,2)$ is empty, and the set $\Sigma_t(H,Q,1)$ is a translate of the set G from Lemma 6.5. Each apex lies on a horizontal geodesic extending a horizontal edge of the square S and is half way around the fiber from the center of this edge. From this description, and from Equations 20, we see that the apices do not move at all as t varies. In other words, we obtain $\Sigma_t(H,Q,k)$ from from $\Sigma_{-1}(H,Q,k)$ by applying the translation $(t+1,0,0)$. It now follows from Lemma 5.5 and Lemma 6.5 that Ξ maps each $c \in \mathcal{S}(H,Q,k)$ into $\Sigma(H,Q,k)$ for $k=1,2$ provided that $\Xi(c)$ lies in a fiber over $[-1+P,P]$. It follows from Lemma 5.5 that $\Xi(\mathcal{S}(H,Q,2)$ does not intersect these fibers at all. ♠

Lemma 7.6 *Let $c \in \mathcal{S}(H,Q,k)$ for some k and suppose that $\Xi(c)$ is contained in a fiber over $T \in [1-P,1]$. Then $\Xi(c) \in \mathcal{S}(H,Q,k)$.*

Proof: For $t \in [1-P,1]$ the analysis is exactly the same, except that $\Sigma_t(H,Q,k)$ is translated in the fiber by (P,P). Were we to have chosen the branch of $[\cdot]_2$ that took values in $(-2,2]$ rather than in $[-2,2)$ we would have proved a version of Lemma 6.5 for sets in the fiber over $T=1$, and our set G would have been translated by (P,P), thanks to the boundary identifications on the fundamental domain boundary coming from the lattice Λ_P. ♠

Lemma 7.7 *Let $c \in \mathcal{S}(H,Q,k)$ for some k and suppose that $\Xi(c)$ is contained in a fiber over $T \in [-1+P, 1-P]$. Then $\Xi(c) \in \mathcal{S}(H,Q,k)$.*

Proof: Let $\pi : X \to \boldsymbol{R}^2$ denote the projection $\pi(T,U_1,U_2) = (U_1,U_2)$. For $t \in [-1+P, 1-P]$ we have

$$\pi(\Sigma_t(H,Q,0)) = \pi(\Sigma_{-1}(H,Q,0) \cap \pi(\Sigma_1(H,Q,0)). \tag{84}$$

$$\pi(\Sigma_t(H,Q,1)) = \pi(\Sigma_{-1}(H,Q,1)\Delta\pi(\Sigma_1(H,Q,1)). \tag{85}$$

$$\pi(\Sigma_t(H,Q,2)) = \pi(\Sigma_{-1}(H,Q,1) \cap \pi(\Sigma_1(H,Q,1)). \tag{86}$$

Here Δ denotes symmetric difference. Figure 7.4 illustrates these equalities. We have taken the left side of Figure 7.2 and re-coloring it so that the different shades show the different translates of the basic set G from Lemma 6.5. The translation $(U_1,U_2) \to (U_1+P, U_2+P)$ carries the white point in Figure 7.4 to the black point. In Figure 7.4, $\Sigma_t(H,Q,1)$ is shown in two different shades of grey and $\Sigma_t(H,Q,2)$ in black. The white set is $\Sigma_t(H,Q,0)$.

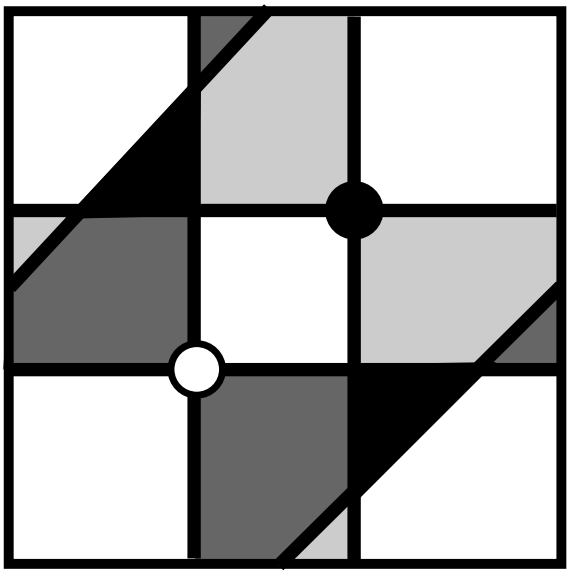

Figure 7.4: $\Sigma(H,P,1)$ (grey) and $\Sigma(H,P,2)$ over a fiber in $[-1+P, 1-P]$.

Now there are 4 cases to consider.

Case 1: Suppose that the south edge of c contains two light points, z_1 and z_2. Suppose that z_1 is the one on the left and z_2 is the one on the right. By Lemma 5.6, there is another instance z_2' of the particle containing z_2 such that $\Xi(z_2') \in \Sigma_{-1}(H, Q, 1)$, and $\Xi(z_2')$ and $\Xi(z_2)$ lie on the same horizontal segment in $[-1, 1]^3$. Similarly, there is another instance z_1' of the particle containing z_1 so that $\Xi(z_1') \in \Sigma_1(H, Q, 1)$, and $\Xi(z_1')$ and $\Xi(z_1)$ lie on the same horizontal segment in $[-1, 1]^3$. But then it follows from Equation 86 that $\Xi(c) \in \Sigma(H, Q, 2)$.

Case 2: Suppose that the south edge of c contains one light point z_1 and one dark point z_2, with z_1 being on the left. This is the same as Case 1, except that $\Xi(z_2') \in \Sigma_{-1}(H, Q, 0)$. But then, by Equation 85, we have $\Xi(c) \in \Sigma(H, Q, 1)$.

Case 3: Suppose that the south edge of c contains one dark point z_1 and one light point z_2, with z_1 being on the left. This is the same as Case 1, except that $\Xi(z_1') \in \Sigma_1(H, Q, 0)$. But then, by Equation 85, we have $\Xi(c) \in \Sigma(H, Q, 1)$.

Case 4: Suppose that the south edge of c contains two dark points. This time we have $\Xi(z_1') \in \Sigma_1(H, Q, 0)$, and $\Xi(z_2') \in \Sigma_{-1}(H, Q, 0)$. Equation 84 tells us that $\Xi(c) \in \Sigma(H, Q, 0)$.

This exhausts all the cases. ♠

This concludes the proof of the Isomorphism Theorem.

8 The PET Equivalence Theorem

8.1 Orientations

In this chapter we deduce the PET Equivalence Theorem from the Isomorphism Theorem. This is mainly just a matter of interpretation.

The tile description of the plaid model allows for the possibility of orienting the loops in the model. There are $12+1$ ways of drawing a directed edge in a square tile which connects up the midpoints of different sides. Aside from the empty tile, the remaining 12 tiles are indexed by ordered 2-element subsets of $\{N, S, E, W\}$. As a first step in proving the PET Equivalence Theorem. we explain the oriented version of our model.

We partition $[0,1] \times \boldsymbol{R}^3$ by thinking of this space as the universal cover of X and then lifting the pieces of the partition. We then quotient out by the index 2 affine subgroup Λ' which, for each parameter P, acts as the lattice generated by

$$(4, 2P, 2P), \qquad (0, 2, 0), \qquad (0, 0, 2). \tag{87}$$

We let $\widehat{X}$ denote this quotient. We think of

$$[0,1] \times [-2,2] \times [-1,1]^2$$

as the fundamental domain for $\widehat{X}$. This turns out to be the most symmetric choice. We can identify X with the middle half of this fundamental domain, namely

$$[0,1] \times [-1,1] \times [-1,1]^2,$$

We enhance the labels on $\widehat{X}$ in the following way:

- For $T \in [-1,1]$ we use the labels as they are ordered in Figure 3.1.
- For $T \in [-2,-1] \cup [1,2]$ we use the labels in the reverse order. So, for instance, the piece labeled NW in Figure 3.1 would be labeled WN in the other half of $\widehat{X}$.

One can see the oriented version in action using my computer program.

8.2 Proof of Oriented Coherence

Theorem 8.1 *The classifying pair $(\widehat{\Xi}_P, \widehat{X}_P)$ produces coherently oriented tilings at all parameters $P \in (0,1)$.*

We will prove this result through a series of smaller lemmas. We will explain the argument in one of 8 cases. The argument works the same in all cases. Define

$$\widehat{X}_{S\downarrow} = \widehat{X}_{ES} \cup \widehat{X}_{WS} \cup \widehat{X}_{NS} \tag{88}$$

as the union of all regions in $\widehat{X}$ which assign tiles that point into their south edge. This set is a finite union of 4 dimensional convex integral polytopes. In a similar way, define $\widehat{X}_{N,\downarrow}$ as the set of all regions which assign tiles that point out of their north edges.

There is an integral affine transformation $\Upsilon : \widehat{X} \to \widehat{X}$ which has the property that

$$\Upsilon \circ \Xi(x,y) = \Xi(x,y-1). \tag{89}$$

From Equation 17, we get

$$\Upsilon(P,\widehat{T},U_1,U_2) = (P,\widehat{T}-2,U_1,U_2-2P) \mod \Lambda. \tag{90}$$

This map is a fiberwise translation. In particular, the image of a finite union of K convex integer polytopes under Υ is again a finite union of K convex integer polytopes.

The statement that every tile which points into the south edge meets a tile below it that points out of the north edge is equivalent to the statement that

$$\Upsilon(\widehat{X}_{S,\downarrow}) = \widehat{X}_{N,\downarrow}. \tag{91}$$

Recall from the description in §3.4 that X is partitioned into 3 zones. So, $\widehat{X}$ is partitioned into 6 zones. More precisely, $\widehat{X}$ is a fiber bundle over a union of 6 integer triangles, and each zone is the preimage of one of the triangles. Each of our sets intersects a zone in a convex integer polytope. Hence $K = 6$.

Say that a *triad* is a triple of parameters $\{(P_i, T_i)\}$ for $i = 1,2,3$ which lies in the interior of one of the 6 triangles in the base space.

Lemma 8.2 *Suppose that Equation 91 holds in the fibers associated to* 6 *triads, one per zone. Then Equation 91 holds everywhere.*

Proof: The two sets in Equation 91 intersect each zone in a convex integer polytope. Let L and R respectively be the intersection of the left and right hand sides of Equation 91 with one of the zones. As we discussed in §3.4, both L and R are intersect each interior fiber in a rectangle. (We mean

a fiber over an interior point of the base.) From this description, we have $L = R$ provided that L and R intersect a triad of fibers in the same way. ♠

Lemma 8.3 *Suppose that the classifying pair $(\widehat{\Xi}_P, \widehat{X})$ produces a coherently oriented tiling at the parameters $p/q = 3/8$ and $p = 4/11$ (corresponding to $P = 6/11$ and $P = 8/15$). Then Equation 91 holds everywhere.*

Proof: First we consider some general parameter p/q. Let $\omega = p + q$. Let $P = 2p/\omega$. Let $\mathcal{C}$ denote the set of centers of the square tiles. Over any fiber F which contains points of $\Xi_P(\mathcal{C})$, we divide F into ω^2 squares of side-length $2/\omega$. As we discussed in §3.5, the image of $\Xi_P(\mathcal{C}) \cap F$ is exactly the set of centers of these little squares.

At the same time, $\widehat{X}_{N,\downarrow}$ intersects F in the segments extending the edges of the little squares. But the translation Υ preserves the division of $\widehat{X}$ into cubes of side length $2/\omega$. Hence $\Upsilon(\widehat{X}_{S,\downarrow})$ also intersects F in the segments extending the sides of the little squares.

It follows from Lemma 3.1 that $\Xi(\mathcal{C}) \cap F$ contains every little square center. Hence, of our two sets disagreed in F, there would be some mismatch of orientations we could see in the tiling. Since the tiling is coherently oriented, there is no mismatch.

The parameters 3/8 and 4/11 are large enough so that the image

$$\Xi_{6/11}(\mathcal{C}) \cup \Xi_{8/15}(\mathcal{C})$$

contains a triad in every zone. ♠

Now we simply inspect the picture for these two parameters and see that the tiling produced is coherent. The parameters involved are so small that there is no round-off error in the calculation.

8.3 Polytope Exchange Transformations

The data for a polytope exchange transformation is two partitions of a polytope Y into smaller polytopes.

$$Y = \bigcup_{i=1}^{N} L_i = \bigcup_{i=1}^{N} R_i. \tag{92}$$

By *partition* we mean that the smaller pieces have pairwise disjoint interiors.

We insist that there is some translation f_i so that $f_i(L_i) = R_i$ for all i. These maps piece together to give an almost-everywhere defined map $F : Y \to Y$. One defines $F(p) = f_i(p)$ provided that p lies in the interior of L_i. The inverse map is defined to be $F^{-1}(q) = f_i^{-1}(q)$ provided that q lies in the interior of R_i.

A variant of this is to consider Y to be a flat manifold. This case really isn't that different from the polytope case, and indeed by refining the partitions we can readily convert between one to the other. One encounters this situation when one considers a circle rotation to be a 2-interval IET. A refinement of the partition introduces new points where the map is not, strictly speaking, defined. However, we will see that this situation has no impact on our main goals. In the irrational case, we will study orbits which are well-defined in either set-up.

For each parameter p/q, we set $P = 2p/(p+q)$, and our space is $\widehat{X}_P$. The partition is given by

$$\widehat{X}_{S\downarrow} \cup \widehat{X}_{W\leftarrow} \cup \widehat{X}_{N\uparrow} \cup \widehat{X}_{E\rightarrow}. \cup \widehat{X}_{\square}. \tag{93}$$

The remaining set $\widehat{X}_{\square}$ is just the complement. These sets have an obvious meaning. We already defined $\widehat{X}_{S\downarrow}$. The set $\widehat{X}_{E,\rightarrow}$ is the union of regions which assign tiles which point into their east edges. And so on. The second partition of $\widehat{X}$ is obtained by reversing all the arrows.

In other words, the pieces in the first partition are understood as the ones which specify tiles according to the edges they point into and the pieces in the second partition are understood as the ones which specify tiles according to the edges they point out of. Both partitions share the regions which assign the empty tile.

We have 5 *curve following maps* $\Upsilon_{\square} : \widehat{X}_{\square} \to \widehat{X}_{\square}$ is the identity, and then $\Upsilon_S : \widehat{X}_{S\downarrow} \to \widehat{X}_{N\downarrow}$. And so on. These maps are all translations on their domain.

There is a natural map on $\mathcal{C}$, the set of centers of the square tiles. We simply follow the directed edge of the tile centered at c and arrive at the next tile center. By construction, $\widehat{\Xi}_P$ conjugates this map on $\mathcal{C}$ to our polyhedron exchange transformation. If we work within the fundamental domain, then $\widehat{\Xi}_P$ is a bijection, by Lemma 3.1. By construction $\widehat{\Xi}_P$ sets up a tautological bijection between the plaid polygons and the set of orbits of points of the form $\widehat{\Xi}(c)$, where $c \in \mathcal{C}$. We call these orbits *special orbits*.

By construction $\widehat{\Xi}_P$ sets up a dynamics-respecting bijection the special orbits and the plaid polygons contained in the fundamental domain, with respect to the parameter p/q.

To get the vector dynamics mentioned in the PET Equivalence Theorem, we assign the vectors $(0,-1)$ to the region $\widehat{X}_{S\downarrow}$, and $(-1,0)$ to $\widehat{X}_{W\leftarrow}$, etc. When we follow the orbit of $\Xi(c)$, we get record the list of vectors labeling the regions successively visited by the point. This gives vectors v_1, v_2, v_3. The vectors c, $c+v_1$, $c+v_1+v_2$, etc. are the vertices of the plaid polygon containing c. This is what we mean by saying that the plaid polygons describe the vector dynamics of the special orbits of the PET. This proves the first statement of the PET Equivalence Theorem.

8.4 Global Picture

Now we turn to the second statement of the PET Equivalence Theorem. We define an *affine polytope exchange* transformation just as above, except that the maps f_i are affine transformations rather than translations. We say that such dynamical system is *fibered* if it is a fiber bundle over some base space such that the maps preserve each fiber and act as ordinary PETs there.

Our total space $\widehat{X}$ is naturally a flat affine manifold, as we discussed (for the two-fold quotient) in §3. The partitions defined in the previous section piece together to give a partition of $\widehat{X}$ into finitely many convex polytopes. The polyhedron exchange maps piece together to give piecewise affine maps of $\widehat{X}$. The definitions make sense even for irrational parameters. Thus $\widehat{X}$ is a fibered piecewise affine polytope exchange transformation, and the fiber over P is $\widehat{X}_P$.

We have

$$\widehat{X} = ([0,1] \times \boldsymbol{R}^3)/\widehat{\Lambda}, \tag{94}$$

where $\widehat{\Lambda}$ is a group of *integral* affine transformations. We say that a convex polytope in $\widehat{X}$ is *integral* if one of its lifts to the universal cover has integer vertices. This definition is independent of lift. By construction, all the polytopes in our partitions are integral. In short, $\widehat{X}$ is a fibered, integral, piecewise affine polytope exchange transformation. This proves the second statement of the PET Equivalence Theorem.

9 Connection to Outer Billiards

9.1 Basic Definitions

Outer billiards is a dynamical system defined on the outside of a compact convex set K. The map is defined like this. One starts with $p_0 \in \boldsymbol{R}^2 - P$ and then defines p_1 so that the line segment $\overline{p_0 p_1}$ is tangent to K at a vertex with bisects this segment, as shown in Figure 9.1.

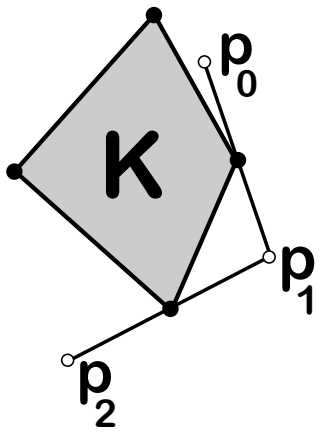

Figure 9.1: Outer billiards on a kite

Of two possible choices for p_1, we choose so that the one finds K on the right as one walks from p_0 to p_1. One defines $p_2, p_3, ...$ in the same way. The map is not defined when p_0 lies on a finite union of rays. This implies that the full orbit $\{p_n\}_{n \in \boldsymbol{Z}}$ is defined for all p_0 in the complement of a countable union of line segments.

Outer billiards was introduced by B. H. Neumann in the late 1950s. See [**N**]. One of the central questions about outer billiards has been: Does there exist a convex set K (not necessarily a polygon) and a point p_0 so that the orbit $\{p_n\}$ exits every compact set? This question, dating from around 1960, is called the Moser-Neumann question. See [**M**]. My monograph [**S1**] has a survey of the known results about this problem. See also [**T1**] and [**T2**]. The main work on this Moser-Neumann problem is contained in [**D**], [**VS**], [**K**], [**GS**], [**G**], [**S1**], [**S2**], and [**DF**].

In [**S2**], I found the first example of a shape with unbounded orbits - the Penrose kite. In [**S1**] I subsequently showed that there are orbits with respect to any irrational kite. Any kite is affinely equivalent to the kite K_A

with vertices

$$(-1,0), \qquad (0,1), \qquad (0,-1), \qquad (A,0), \qquad A \in (0,1). \tag{95}$$

K_A is rational if and only if $A \in \boldsymbol{Q}$. Outer billiards on K_A preserves the infinite family of horizontal lines

$$\Lambda = \boldsymbol{R} \times \boldsymbol{Z}_1. \tag{96}$$

Here $\boldsymbol{Z}_1$ is the set of odd integers. Let ψ_A denote the square of the outer billiards map, restricted to Λ.

9.2 The Arithmetic Graph

One of the main tools I used in [**S1**] to understand ψ_A was the *arithmetic graph*. Let Ψ_A denote the second iterate of the first return map of ψ_A to the two lines

$$\Upsilon = \boldsymbol{R} \times \{-1,1\} \subset \Lambda. \tag{97}$$

(The first return map moves points a long distance, but the second return map is close to the identity.) The set Υ is shown in Figure 9.2. If we choose some "offset" $t \in \boldsymbol{R}_+$, as well as integers m_0, n_0, then it turns out that

$$\Psi_A\Big(2m_0A + 2n_0 + t, (-1)^{m_0+n_0}\Big) = \Big(2m_1A + 2n_1 + t, (-1)^{m_1+n_1}\Big) \tag{98}$$

for some other pair of integers m_1, n_1 which depends on A and t.

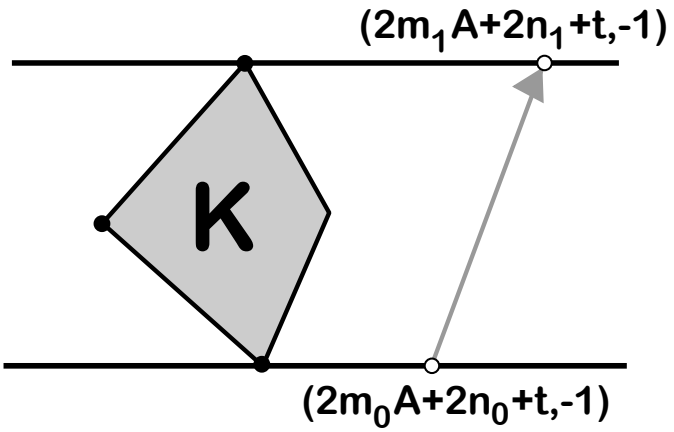

Figure 9.2: The second return map to Υ.

To the point

$$p_0 = \Big(2m_0A + 2n_0 + t, (-1)^{m_0+n_0}\Big). \tag{99}$$

we have the orbit $\{p_k\}$ and, by the above correspondence, the sequence of integers $\{(m_k, n_k)\}$. These integers define a polygonal path whose vertices lie in the integer lattice - i.e. a *lattice path*. This lattice path is called the *arithmetic graph* of the orbit.

I proved in [**S1**] that these lattice paths are always embedded. It we fix t and consider the orbits of all possible points of the form given in Equation 99, we get a disjoint union of embedded lattice paths. When $A = p/q$ is rational, it turns out that Υ is partitioned into intervals of size $2/q$ which are permuted by Ψ_A. In this case, the choice $t = 1/q$ is a canonical choice; it corresponds to the centers of these intervals. The corresponding union of lattice paths describes every special orbit at the same time. We call this union of all arithmetic graphs the *arithmetic landscape*, and we denote it by $\Gamma(p/q)$.

9.3 Quasi-Isomorphism Conjecture

It turns out that $\Gamma(p/q)$ is invariant under a certain lattice acting on $\boldsymbol{Z}^2$. The lattice is generated by vectors V and $(p+q)W$, where

$$V = (q, -p), \qquad W = \Big(\frac{2pq}{p+q}, \frac{2pq + q^2 - p^2}{p+q}\Big). \tag{100}$$

A fundamental domain for the action is a certain parallelogram with sides parallel to V and $(p+q)W$ and southwest corner $\Theta(p,q)$. The point $\Theta(p,q)$ is given by a rather complicated formula, which runs like this:

- Let p'/q' be the unique even rational with $|pq' - p'q| = 1$.
- Let $x = (q - q')/2$ and $y = -xp/q$.
- If $p'/q' > p/q$ let $x = -x$ and $y = -y$.
- If $x > 0$ let $x = x - q$ and $y = y + 0$.

Then $\Theta = (x, y)$.

The *first block* of the big parallelogram has southwest corner Θ and sides parallel to V and W. Call this parallelogram Ω_0. It turns out that none of

the polygons in the arithmetic landscape cross the boundaries of Ω_0. This is about half the content of our Hexagrid Theorem in the case when pq is even. (In fact we only proved the odd case.)

There is an affine transformation $T_{p/q}$ which maps the first block $B_0 = [0, p+q]^2$ to Ω_0. Figure 1.3 shows $T_{p/q}^{-1}(\Gamma_{3/8})$ superimposed over the union of plaid polygons for the parameter $3/8$ contained in B_0. One can see similar pictures for other parameters using my computer program. We can define the other $p+q-1$ blocks by moving Ω_0 parallel to itself. Our affine map $T_{p/q}$ carries the fundamental domain for the plaid model to the fundamental domain for the arithmetic graph.

Conjecture 9.1 (Quasi-Isomorphism) *There is a bijection between the polygons of $T_{p/q}^{-1}(\Gamma_{p/q})$ in the fundamental domain and the polygons of the plaid model at p/q in the fundamental domain, so that each polygon in the one model is within a 2-tubular neighborhood of the corresponding polygon in the other.*

One might wonder what the Quasi-Isomorphism Conjecture has to do with the dynamics. Here is a consequence of the Quasi-Isomorphism Conjecture (which we will flesh out when we prove the conjecture). Let $A = p/q$ as above. Recall that Ψ_A is the second return map to Υ. We define two orbits of Ψ_A to be *equivalent* if reflection in the x-axis swaps them. Two equivalent orbits are essentially the same. All the Ψ_A orbits come in pairs like this.

Corollary 9.2 *Let $A = p/q$ with pq even. Let π_1 be projection onto the x-axis. There is a bijection between the plaid polygons in $[0, \infty] \times [0, p+q]$ and the equivalence classes of Ψ_A orbits. The bijection is such that for each polygon γ, the image $\pi_1(\gamma)$, when parametrized by arc length, remains vertex by vertex within 5 units of the corresponding Ψ_A orbit.*

In other words, the plaid model says all there is to know about the coarse geometry and arithmetic of the special outer billiards orbits on kites.

10 References

[**DeB**] N. E. J. De Bruijn, *Algebraic theory of Penrose's nonperiodic tilings*, Nederl. Akad. Wentensch. Proc. **84**:39–66 (1981).

[**DF**] D. Dolyopyat and B. Fayad, *Unbounded orbits for semicircular outer billiards*, Annales Henri Poincaré **10** (2009) pp 357-375

[**G**] D. Genin, *Regular and Chaotic Dynamics of Outer Billiards*, Pennsylvania State University Ph.D. thesis, State College (2005).

[**GS**] E. Gutkin and N. Simanyi, *Dual polygonal billiard and necklace dynamics*, Comm. Math. Phys. **143**:431–450 (1991).

[**H**] W. Hooper, *Renormalization of Polygon Exchange Transformations arising from Corner Percolation*, Invent. Math. **191.2** (2013) pp 255-320

[**Ko**] Kolodziej, *The antibilliard outside a polygon*, Bull. Pol. Acad Sci. Math. **37**:163–168 (1994).

[**M**] J. Moser, *Is the solar system stable?*, Math. Intelligencer **1**:65–71 (1978).

[**N**] B. H. Neumann, *Sharing ham and eggs*, Summary of a Manchester Mathematics Colloquium, 25 Jan 1959, published in Iota, the Manchester University Mathematics Students' Journal.

[**S1**] R. E. Schwartz, *Outer Billiard on Kites*, Annals of Math Studies **171** (2009)

[**S2**] R. E. Schwartz, *Unbounded Orbits for Outer Billiards*, J. Mod. Dyn. **3**:371–424 (2007).

[**T1**] S. Tabachnikov, *Geometry and billiards*, Student Mathematical Library 30, Amer. Math. Soc. (2005).

[**T2**] S. Tabachnikov, *Billiards*, Société Mathématique de France, "Panoramas et Syntheses" 1, 1995

[**VS**] F. Vivaldi and A. Shaidenko, *Global stability of a class of discontinuous dual billiards*, Comm. Math. Phys. **110**:625–640 (1987).